

## NEW DISTANT COMPANIONS TO KNOWN NEARBY STARS. II. FAINT COMPANIONS OF *HIPPARCOS* STARS AND THE FREQUENCY OF WIDE BINARY SYSTEMS.

SÉBASTIEN LÉPINE, & BETHANY BONGIORNO<sup>1</sup>

Department of Astrophysics, Division of Physical Sciences, American Museum of Natural History, Central Park West at 79th Street, New York, NY 10024, USA

To appear in the *Astronomical Journal*. MS #205339.

### ABSTRACT

We perform a search for faint, common proper motion companions of *Hipparcos* stars using the recently published *LSPM-north catalog* of stars with proper motion  $\mu > 0.15'' \text{ yr}^{-1}$ . Our survey uncovers a total of 521 systems with angular separations  $3'' < \Delta\theta < 1500''$ , with 15 triples and 1 quadruple. Our new list of wide systems with *Hipparcos* primaries includes 130 systems identified here for the first time, including 44 in which the secondary star has  $V > 15.0$ . Our census is statistically complete for secondaries with angular separations  $20'' < \Delta\theta < 300''$  and apparent magnitudes  $V < 19.0$ . Overall, we find that at least 9.5% of nearby ( $d < 100 \text{ pc}$ ) *Hipparcos* stars have distant stellar companions with projected orbital separations  $s > 1,000 \text{ AU}$ . We observe that the distribution in orbital separations is consistent with Öpik's law  $f(s)ds \sim s^{-1}ds$  only up to separation  $s \approx 4,000 \text{ AU}$ , beyond which it follows a more steeply decreasing power law  $f(s)ds \sim s^{-l}ds$  with  $l = 1.6 \pm 0.1$ . We also find that the luminosity function of the secondaries is significantly different from that of the single stars field population, showing a relative deficiency in low-luminosity ( $8 < M_V < 14$ ) objects. The observed trends suggest either a formation mechanism biased against low-mass companions, or a disruption over time of systems with low gravitational binding energy.

*Subject headings:* astrometry — stars: double — stars: kinematics — Galaxy: kinematics and dynamics — solar neighborhood

### 1. INTRODUCTION

Stellar systems composed of two or more stars (binaries, multiples) are known to exist in a wide range of configurations. They range from tight spectroscopic binaries with orbital periods of days to years and separations under 10 AU (Halbwachs *et al* 2003), to marginally bound *wide binaries* with orbital periods  $> 10^5 \text{ yr}$  and separations up to 20,000 AU (0.1 parsec) or more (Chanamé & Gould 2004). The frequency of stellar binaries, and the statistics of their physical properties (periods, mass ratios, eccentricities) provide constraints on theoretical models of star formation (Bate 2000; Klein *et al.* 2003; Delgado-Donate *et al.* 2004; Goodwin & Kroupa 2006).

Binaries are very common in the Galaxy, with various estimates of their frequency hovering around 50% of all stellar systems. The distribution in orbital periods  $P$  has been estimated over several orders of magnitude, from days to millions of years, in the classical papers by Duquenois & Mayor (1992) and Fisher & Marcy (1992). The orbital period distribution of spectroscopic doubles was also re-estimated more recently by Goldberg, Mazeh, & Latham (2003). There appears to be a general consensus in the literature for an orbital period distribution which is uniform in  $\log P$  over several orders of magnitude. The orbital period distribution is traditionally modeled with a power law  $f(P)dP \sim P^{-1}dP$ , sometimes referred to as *Öpik's law* after Öpik (1924); an equivalent form uses the orbital separation of the components  $f(S)dS \sim S^{-1}dS$ . This empirical law breaks down both at very short orbital periods (Goldberg, Mazeh, & Latham 2003), and at large orbital separations (Chanamé & Gould 2004), where the binary frequency is found to drop.

The observed distribution of *wide binaries* is of particular interest, because the low binding energy of these systems makes them susceptible to disruption. Theoretical models suggest that marginally bound systems in the Galactic disk will dissolve over timescales comparable with the age of the Galaxy through repeated, separate encounters with field stars, giant molecular clouds, or hypothetical dark matter bodies (Retterer & King 1982; Weinberg, Shapiro, & Wasserman 1987; Mallada & Fernandez 2001). Since the probability of a system to become disrupted increases with component separation, it is expected that an evolved population of wide binaries will exhibit a break in its distribution at large orbital separations. Hence even a population whose initial distribution strictly following Öpik's law ( $f(S)dS \sim S^{-1}dS$ ) will end up with a truncated distribution, with  $f(S)$  breaking down to a steeper power law ( $f(S)dS \sim S^{-l}dS$ , with  $l > 1$ ) beyond some orbital separation limit. The specific form of  $f(S)$  will be a function of both the age and interaction history of the binary population under study. Samples of wide binaries can thus be used as probes of the environments of various populations of objects. To investigate these statistical effects, it is however desirable to assemble *large samples* of wide binary systems. Much can also be learned by assembling and comparing samples drawn from a variety of populations and stellar subtypes (e.g. Abt 1983; Poveda & Allen 2004).

The classical method to find wide binaries is to search for pairs of stars with small angular separations on the sky. The main problem is to distinguish between *physical pairs*, i.e. genuine resolved binary stars, and *optical pairs*, which are chance alignments of unrelated stars along the line of sight. While all physical binaries should ultimately be confirmed through the detection of their orbital motion, this is generally impractical for wide binaries with orbital periods of  $10^4$  years or longer. Wide binaries are thus generally identified based of

<sup>1</sup> National Science Foundation Research Experience for Undergraduate intern.

probability arguments. Besides angular separations, other observables are useful in assessing the status of candidate wide binaries. Parallax measurements are perhaps the most useful, when they exist; orbital separations are expected to be  $\lesssim 1$  pc, so both components should have very nearly identical parallaxes. Wide binaries are also expected to have orbital velocities  $< 1$  km s $^{-1}$ , so their radial velocities should be nearly identical, as well as their proper motion vectors. While radial velocities are efficient at separating out physical and optical pairs at any distance range, parallaxes and proper motions are most useful at small radial distances, where their relative accuracies are higher.

One identifies in the literature two distinct approaches in identifying wide binaries. One approach attempts to identify distant wide binaries in deep imaging surveys using statistical arguments based on angular separations alone. A classical example is the two-point correlation method elaborated by Bahcall & Soneira (1981). Their analysis of deep images of North Galactic Pole demonstrated an excess of pairs with small angular separations, compared to what one would expect from a random distribution of single stars. Radial velocity measurements have been used to confirm the binary status of the candidates (Latham *et al.* 1984). This, and other similar surveys (Garnavich 1988; Saarinen & Gilmore 1989; Gould *et al.* 1995), have however yielded only limited samples of wide binaries.

The second, more successful, approach is based on a search for wide binaries among catalogs of stars with large proper motions. In such catalogs, wide binaries are expected to be found as *common proper motion* (CPM) doubles. This method has been expanded to a considerable extent by W. J. Luyten (1988). His *LDS Catalogue*<sup>2</sup> (Luyten 1987), contains over 6,200 wide binaries, with proper motions  $\mu > 0.1''$  yr $^{-1}$ . Searching for wide binaries among high proper motion stars has several advantages. Such stars tend to be relatively nearby ( $d \lesssim 100$  pc), which means that wide binaries with orbital separations as small as  $a \gtrsim 10^2$  AU will generally be resolved in most imaging surveys, including archived photographic plate. The proximity of the high proper motion population also makes it easier to identify *intrinsically faint* companions, such as M dwarfs or brown dwarfs. High proper motion stars are also generally within range of accurate parallax measurements, which ultimately provide the most stringent test of the binary star status of the components.

Unfortunately, a complete catalog of all the high proper motion stars surveyed for CPM companions was never published by Luyten, leaving no data on the parent population. In particular, it must be emphasized that the LDS catalog is not a subsample of the *NLTT catalog*<sup>3</sup> (Luyten 1979); the NLTT catalog compiles only the fastest stars identified by Luyten ( $\mu > 0.18''$  yr $^{-1}$ ) and  $\approx 69\%$  of the LDS pairs have proper motions below the NLTT limit. Other limitations of both the LDS and NLTT catalogs include (1) a limited precision in the tabulated proper motions (Gould & Salim 2003) which leaves significant uncertainties on some of the pairings, and (2) a photographic magnitude system ( $m_{pg}, m_r$ ) which does not yield reliable photometric distances for red dwarfs (Weis 1984). Both the LDS and NLTT catalogs also suffer from incompleteness, particularly in areas of high stellar densities such as in Milky Way fields, and also at faint ( $V \gtrsim 17$ ) magnitudes. Neverthe-

less, the LDS and NLTT catalogs still provide ample opportunities to conduct additional surveys and analyses of wide binary systems, and one can argue that they have remained under-utilized in this respect. A successful use of the Luyten catalogs is demonstrated by Allen, Poveda, & Herrera (2000), who surveyed a well-defined sample of  $\approx 1,200$  high proper motion objects, identifying and analyzing 122 CPM companions.

A more systematic search for wide binaries using the Luyten catalogs was made possible with the release of the revised NLTT catalog (rNLTT) assembled by Salim & Gould (2003). The rNLTT is based on the re-identification of NLTT stars in the USNO-A catalog (Monet *et al.* 1998) and in the 2MASS *Second Incremental Release* (Skrutskie *et al.* 1997). This fixed some of the main limitations of the NLTT by providing significantly more accurate positions, proper motions, and magnitudes. Additionally, the new optical-to-infrared colors make it possible to separate out white dwarfs, disk dwarfs, and halo subdwarfs in a reduced proper motion diagram (Salim & Gould 2002). A complete analysis of the rNLTT yielded an expanded list of 1124 CPM doubles Chanamé & Gould (2004), including clearly defined samples of wide binaries from both the local disk and local halo populations. These samples suggest that the distribution in orbital separations in both disk and halo wide binaries is consistent with a power law distribution of the form  $f(S)dS \sim S^{-l}dS$  with  $l \simeq 1.6$ , significantly different from Öpik's law ( $l = 1$ ).

Perhaps the most interesting CPM doubles are those for which at least one component is a star listed in the *Hipparcos* catalog. A systematic search of both the NLTT and rNLTT by Gould & Chanamé (2004) – hereafter GC04 – has yielded 424 such pairs. The identification of a distant, faint companion to a *Hipparcos* star automatically yields a high-quality parallax for the faint secondary, which can be critical in mapping the color-magnitude relationship of low-luminosity stars (Lépine 2005). But perhaps the most interesting feature for the investigation of wide binaries is that an accurate parallax also yields an accurate measurement of the projected *physical separation* between the two components, which can be more directly compared with theoretical models.

The new LSPM-north catalog of stars with proper motion  $\mu > 0.15''$  yr $^{-1}$  (Lépine & Shara 2005) now provides a fresh opportunity to expand the census of CPM doubles, including systems with *Hipparcos* primaries. The LSPM-north catalog<sup>4</sup> is based on a re-analysis of the Digitized Sky Survey (DSS) with the SUPERBLINK software, which used an image-subtraction algorithm to achieve a high detection rate for stars with significant proper motions. The catalog covers the entire hemisphere north of the J2000 celestial equator (Decl. $>0$ ). It is estimated to be  $> 95\%$  complete over the entire northern sky down to an apparent magnitude  $V = 19$ . In fields at high galactic latitude ( $|b| > 20$ ), its completeness is  $> 99\%$ . The LSPM-north also has a lower proper motion limit than the NLTT catalog ( $0.15''$  yr $^{-1}$ , compared with  $0.18''$  yr $^{-1}$ ). Nearly half (30,616) of its 61,977 recorded high proper motion stars are not listed in the NLTT. Just like the rNLTT, the LSPM-north provides more accurate positions, proper motions, and magnitudes, and also gives optical-to-infrared colors.

In paper I, we demonstrated the potential for using the SUPERBLINK database to find new CPM companions, report-

<sup>2</sup> CDS-ViZier catalog number I/130

<sup>3</sup> CDS-ViZier catalog number I/98A

<sup>4</sup> CDS-ViZier catalog number I/298

ing the discovery of 5 new companions of known nearby stars (Lépine, Shara, & Rich 2002a). In this second paper, we capitalize on the very high completeness of the LSPM-north to obtain a statistically complete census of faint CPM companions to *Hipparcos* stars. Our methodology for identifying CPM doubles is described in §2, our resulting census of CPM pairs is presented in §3 and 4, a statistically complete sample of wide binaries is defined and analyzed in §5, the main results are summarized in the conclusion (§6).

## 2. IDENTIFICATION OF COMMON PROPER MOTION DOUBLES

### 2.1. *Genuine CPM doubles versus chance alignments*

Common proper motion (CPM) doubles are, by definition, resolved pairs of stars which have similar proper motions, both in magnitude and orientation. They typically have angular separations ranging from several arcseconds to several arcminutes. They are assumed to be the resolved components of wide binary systems. As such, they are also expected to orbit around their common center of mass and display orbital motion. CPM doubles are thus not expected to have *identical* proper motion vectors, since the orbital motion will result in a small relative proper motion between the components of the pair. In most cases, however, the orbital period will be large enough ( $\gtrsim 10^4$  yr) that the relative proper motion between the stars will be negligible on timescales of years to decades. Modern proper motion measurements will thus be comparable to within the measurement errors. Pairs of high proper motion stars resulting from a chance alignment, on the other hand, will generally have different proper motions, although there remains a small probability that a few will, by chance, also have similar proper motions (although they may lie at very different distances). The formal identification of a CPM pair as a wide binary thus requires one to weight in the probability for a common proper motion pair to be a chance alignment.

Consider two stars at angular positions  $\alpha_1, \delta_1$  and  $\alpha_2, \delta_2$ , where  $\alpha$  refers to the Right Ascension and  $\delta$  to the Declination on the sky. These stars have proper motions  $\mu_{\alpha_1}, \mu_{\delta_1}$  and  $\mu_{\alpha_2}, \mu_{\delta_2}$ . For small angles of separation between stars 1 and 2, we can approximate the angular separation  $\Delta\theta$  between the stars as:

$$\Delta\theta \simeq ((\alpha_1 - \alpha_2)^2 \cos^2(\delta_1) + (\delta_1 - \delta_2)^2)^{\frac{1}{2}}. \quad (1)$$

We can also define  $\Delta\mu$  as the magnitude of the difference between the proper motion vectors:

$$\Delta\mu = ((\mu_{\alpha_1} - \mu_{\alpha_2})^2 + (\mu_{\delta_1} - \mu_{\delta_2})^2)^{\frac{1}{2}}. \quad (2)$$

Each pair can thus be represented in a  $(\Delta\theta, \Delta\mu)$  phase space. For large numbers of pairs, one can then statistically determine the probability for a pair to be a chance alignment by comparing the actual distribution of pairs in the  $(\Delta\theta, \Delta\mu)$  phase space with a model of the distribution expected from chance alignments.

The expected distribution of chance alignments in  $(\Delta\theta, \Delta\mu)$  phase space is very hard to modelize analytically for a proper motion catalog such as the LSPM-north. One complication is that the distribution of high proper motion stars is not uniform in  $\alpha$  and  $\delta$  with some regions of the sky being more densely populated than others (Lépine & Shara 2005). The distribution in proper motions  $\mu_{\alpha}, \mu_{\delta}$  is also not uniform. Proper motion vectors have preferred orientations in some parts of the sky, most notably because of the asymmetric drift of thick disk and halo stars, as well as from the Solar motion relative to

the local standard of rest, both effects resulting in preferred orientations of the proper motion vectors in specific parts of the sky. Also, the density of objects increases as the proper motion decreases, with very high proper motion stars being rare and low proper motion stars more common.

It is however possible to obtain an empirical model of the density of chance alignments in  $\Delta\theta, \Delta\mu$  phase space. One can picture the calculation of all the  $\Delta\theta$  as a comparison between the positions of all stars in two sets of objects: set #1 with positions  $\alpha_1, \delta_1$ , and set #2 with positions  $\alpha_2, \delta_2$ . We calculate the angular distance separating each individual object in set #2 from each individual object in set #1. Assuming there are  $n_1$  objects in set #1 and  $n_2$  objects in set #2, then we have  $n_1 \times n_2$  pairings. What we are interested in is the special case where the primary star is a *Hipparcos* object. Set #1 is thus the subset of LSPM-north stars with a *Hipparcos* counterpart (4,839 objects), while subset #2 comprises the entire LSPM-north catalog (61,976 objects).

It is possible to modify the dataset and simulate a situation where no genuine CPM pairs would be found, only chance alignments. Let's redefine the angular separation  $\Delta\theta$  as:

$$[\Delta\theta]_{sim} = ((\alpha_1 - [\alpha_2 - \Theta])^2 \cos^2(\delta_1) + (\delta_1 - \delta_2)^2)^{\frac{1}{2}}. \quad (3)$$

This is equivalent to displacing all stars in set #2 by an angle  $\Theta$  in the direction of Right Ascension, prior to calculating angular separations. This procedure effectively eliminates all pairings of genuine CPM doubles (since the second star of the pair is now moved out the way by some angular distance  $\Theta$ ) while leaving intact the statistics of the chance alignments. The procedure can be illustrated with a ballroom analogy. Imagine a crowd of men and women attending a dance function in a large ballroom. Assume that a few of the attendees are married couples, while the rest are singles. Let's say initially all the dancers are scattered around the ballroom at random, but with all the married couples holding hands. People would be found in pairs, some because they are married couples, but other simply by chance. At a specified time, an announcer commands all the men to walk ten steps to their right. After this, new pairings of people would have been made, but this time none of them would be married couples, all would be chance pairings. If we were to calculate how many pairs there were initially, and subtract out the number of pairs after the move, then we would have a good estimate of how many married couples are attending the dance.

The distribution of all pairs in the  $\Delta\theta_{sim}, \Delta\mu$  thus effectively simulates a distribution of pairs in the LSPM-north catalog *as if there were no CPM doubles in it*. The displacement angle  $\Theta$  should be large enough that all CPM doubles are well separated, i.e., larger than the typical angular separation between CPM pairs. However,  $\Theta$  should not be too large because we need to simulate pairing made within areas of the sky that have similar densities and proper motion systematics. We use values of  $\Theta$  between 1 and 5 degrees.

In Figure 1, we compare the distribution in  $\Delta\theta, \Delta\mu$  phase space for LSPM-North pairs with distributions of pairs in the simulated  $\Delta\theta_{sim}, \Delta\mu$  phase space. The left panels show the distribution of pairs with *Hipparcos* primaries, while the right panels shows simulations calculated with  $\Theta = 1$  degree. The distributions are split in three different groups, depending on the mean proper motion  $\mu$  of the pairs,  $0.15''\text{yr}^{-1} < \mu < 0.25''\text{yr}^{-1}$  (top),  $0.25''\text{yr}^{-1} < \mu < 0.35''\text{yr}^{-1}$  (middle), and  $0.35''\text{yr}^{-1} < \mu < 0.45''\text{yr}^{-1}$  (bottom). The panels to the right display the results of the chance alignment simulations (i.e.

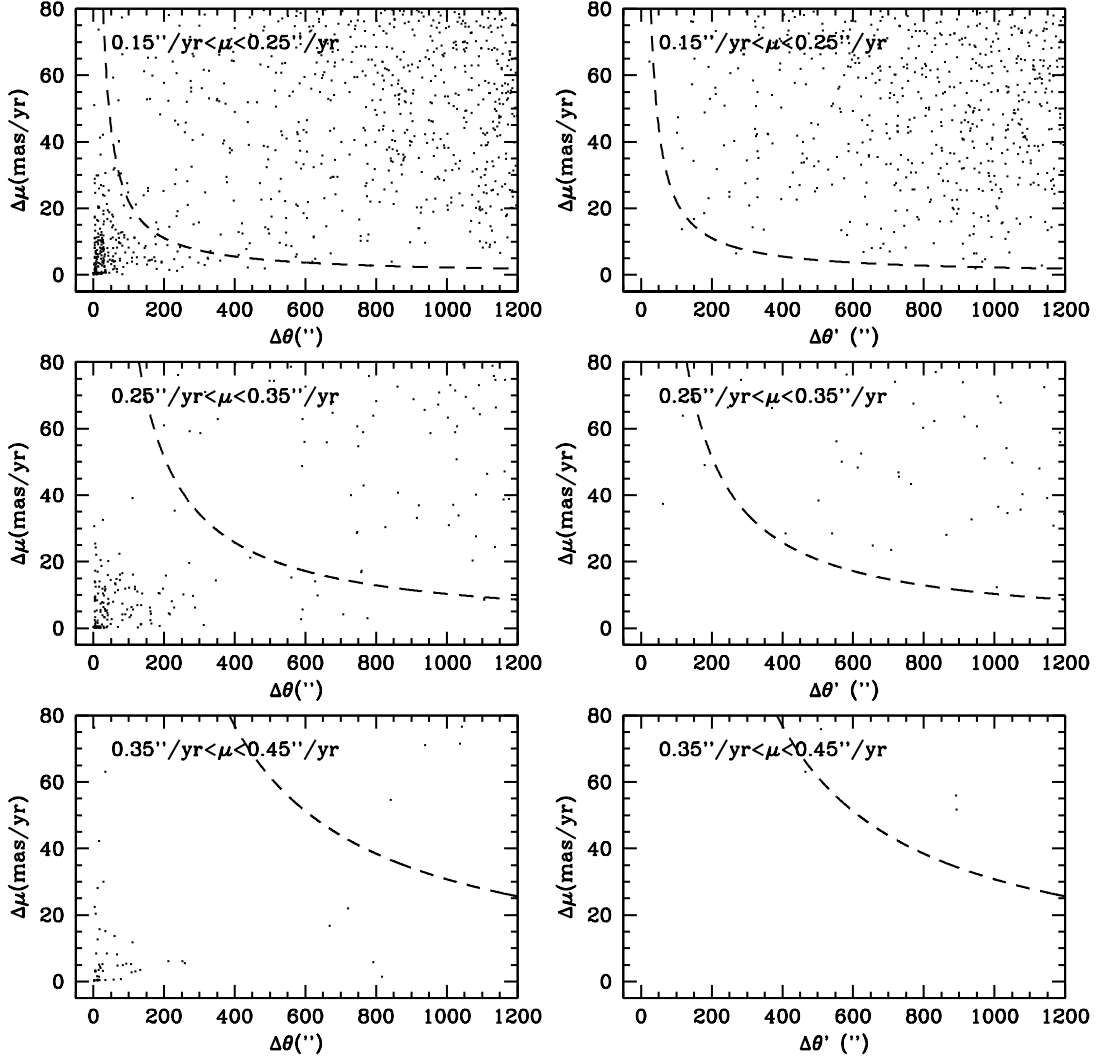


FIG. 1.— Left panels: observed difference in proper motion  $\Delta\mu$  versus angular separation  $\Delta\theta$  for pairs of stars in the LSPM-north catalog with a *Hipparcos* primary. Distributions are shown for three different ranges of absolute proper motion (see labels); pairs of stars with very high proper motions are much rarer because their angular density on the sky is significantly lower. Right panels: simulations of  $\Delta\mu$ ,  $\Delta\theta$  distributions for a catalog of high proper motion stars in which no wide binaries are present, and pairs occur only from chance alignments (see text). The overdensity at small values of  $\Delta\theta$  and  $\Delta\mu$ , in the distribution of observed pairs, are clearly due to wide binary systems, as it cannot be reproduced by chance alignments alone. The dashed lines show the approximate location of our adopted limits for the selection of candidate wide binary systems.

with set #2 translated by an angle  $\Theta$ ), and for comparable ranges of  $\mu$ .

The most striking difference between the data and the simulations are the number of pairs found in the lower left corner of each diagram, corresponding to small angular separations *and* small proper motion differences. Very few pairs are found in the simulations, but the data shows a large concentration of objects in that range. This concentration of objects in the data can only be interpreted as the signature from a population of common proper motion binaries. Pairs of stars found in that region of the parameter space are thus most likely to be genuine physical doubles. The density of chance alignments, however, progressively increases for larger values of  $\Delta\theta$  and  $\Delta\mu$ . There exists a limit beyond which the density of chance alignment pairs exceeds that of the CPM doubles. This limit can be used to objectively define a search area for wide binary systems.

## 2.2. Objective identification of CPM doubles

The distribution of high proper motion stars is locally uniform in  $\alpha, \delta$ , so the probability of having a chance alignment, for small values of  $\Delta\theta$ , is directly proportional to  $\Delta\theta$ . On first order, one also expects the probability of a chance alignment to increase proportionally to  $\Delta\mu$ , again for small values of  $\Delta\mu$ . Thus, for small values of both  $\Delta\theta$  and  $\Delta\mu$  the probability of a chance alignment is expected to be proportional to  $\Delta\mu\Delta\theta$ . In the LSPM-North catalog, the distribution of high proper motion stars empirically follows  $N(\mu)d\mu \simeq \mu^{-2.8}d\mu$ , where  $\mu = \sqrt{(\mu_\alpha)^2 + (\mu_\delta)^2}$ . From that, we infer that the number density of chance alignments  $N_{sim}$  in  $\Delta\theta, \Delta\mu$  phase space must follow:

$$N_{sim}(\Delta\theta, \Delta\mu) \simeq \mu^{-3.8} \Delta\theta \Delta\mu \quad (4)$$

for small values of  $\Delta\theta$  and  $\Delta\mu$ .

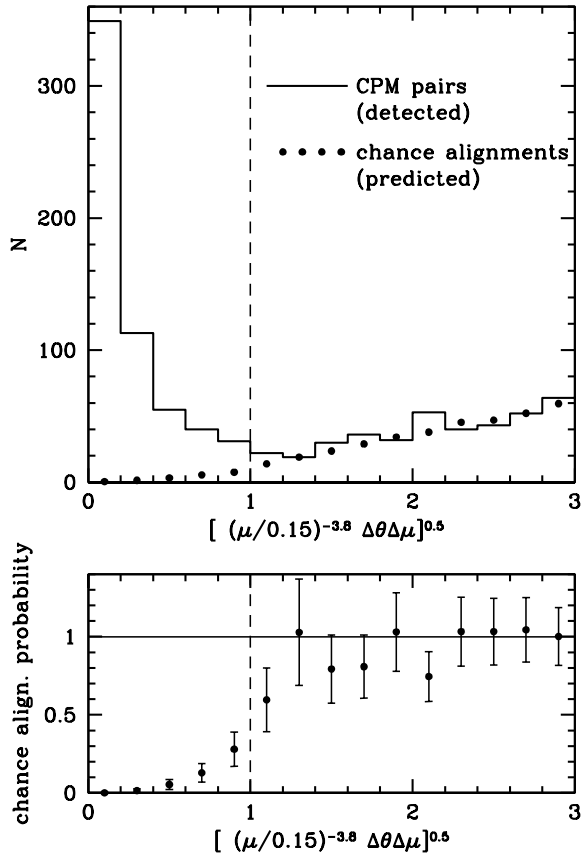


FIG. 2.— Top: comparison between the number density of common proper motion pairs in the LSPM-north catalog (histogram) and the predicted number density of chance alignments, based on our simulations (filled circles). Bottom: ratio between the number of predicted chance alignment and the number of pairs found, giving the probability for a CPM pair to be a chance alignment. The dashed line marks the adopted detection limit for CPM doubles.

To determine the range within which a data pair is most likely to be a CPM double, we define the variable:

$$\Delta X = [(\mu/0.15)^{-3.8} \Delta\theta\Delta\mu]^{0.5}, \quad (5)$$

which includes a normalization of the proper motions to the lower limit of the LSPM-north catalog ( $0.15'' \text{ yr}^{-1}$ ). This new variable is deliberately set up so that the number density of chance alignment pairs increases *linearly* with  $\Delta X$  (hence the square root in Eq. 5). This helps in modeling the contribution from chance alignments, whose density should increase linearly with  $\Delta X$ . We compare the number density distribution of pairs  $N_{dat} = N_{dat}(\Delta X)$  in the data with the mean distribution of simulated, chance alignment pairs  $N_{sim} = N_{sim}(\Delta X)$ , averaged from 20 different simulations. The result is displayed in Figure 2. For small values of  $\Delta X$ , corresponding to small angular distances  $\Delta\theta$  and/or small differences in proper motion  $\Delta\mu$ , one finds that  $N_{dat} \gg N_{sim}$ , which means that there is a high probability for any pair found in that range to be a CPM double. We find that  $N_{sim}$  increases linearly with  $\Delta X$ , as expected, while  $N_{dat}$  steadfastly decreases when  $\Delta X$  increases, up to a point where  $N_{sim}$  begins to dominate. The bottom panel in Figure 2 estimates the probability for a pair to be a chance alignment, as a function of the variable  $\Delta X$ . We find that beyond  $\Delta X = 1$  the probability of a pair to be a chance alignment exceeds 50%. We thus use  $\Delta X = 1$  as the

upper limit in our search for CPM doubles.

We select as wide binary candidate any pair for which  $\Delta X < 1$ , which is equivalent to selecting pairs which satisfy the condition:

$$\Delta\theta\Delta\mu < (\mu/0.15)^{3.8} \quad (6)$$

where  $\Delta\theta$  is expressed in seconds of arc, and  $\Delta\mu$  is in seconds of arc per year. The location of this boundary is illustrated in figure 1 for  $\mu = 0.2'' \text{ yr}^{-1}$  (top),  $\mu = 0.3'' \text{ yr}^{-1}$  (middle), and  $\mu = 0.4'' \text{ yr}^{-1}$  (bottom). Note that the boundary is a function of the mean proper motion ( $\mu$ ) of the pair, which means that pairs with large proper motions are selected over a larger range in  $\Delta\theta$  and  $\Delta\mu$ .

The boundary rises to high values of  $\Delta\mu$  at very small angular separations, setting an unrealistically high limit for the detection of wide binaries, whose proper motions should be very similar in any case. We thus add the following constraint:

$$\Delta\mu < 100 \text{ mas}. \quad (7)$$

This large, arbitrary limit ensures that no pairs with very different proper motions will make the cut, even if they happen to have very small angular separations. The majority of pairs found in the LSPM-north are at distances  $d > 10 \text{ pc}$ , and have projected separations  $s > 100 \text{ AU}$  (see §3,4 below); a difference in proper motion  $\Delta\mu > 100 \text{ mas}$  would imply an orbital velocity  $v_{orb} > 5 \text{ km s}^{-1}$  which would be unrealistically large for any system with  $s > 100 \text{ AU}$ . We also set an upper limit to the range of angular separations:

$$\Delta\theta < 1,500''. \quad (8)$$

This limits the search to a reasonable range in  $\Delta\theta$ . Beyond this limit, the constraints on  $\Delta\mu$  from Eq.7 become so stringent that the allowed range in  $\Delta\mu$  falls well below the measurement errors, thus losing all practicality.

The search area bounded by Eqs.6,7,8 should include the vast majority of genuine wide binaries, with minimal contamination from chance alignment pairs. A small level of contamination is still expected, particularly for pairs selected near the boundaries. Based on our simulations of chance alignments, we estimate the contamination in the entire search area to be  $\approx 10$  pairs, or  $< 2\%$  of the total sample.

### 3. WIDE BINARIES WHERE BOTH THE PRIMARY AND SECONDARY ARE HIPPARCOS STARS

#### 3.1. Proper motion identification

Using the selection method discussed above, we searched the LSPM-north catalog for CPM binaries in which both the primary and secondary (and tertiary) are *Hipparcos* stars. We identified a total of 168 such CPM pairs with angular separations  $3'' < \Delta\theta < 1,200''$ , arranged into 158 doubles and 5 triples. Figure 3 shows the distribution in  $\Delta\theta, \Delta\mu$  for the 163 systems selected as most likely to be wide binaries/multiples (open and filled circles). Fig.3 also shows the  $\Delta\theta, \Delta\mu$  distribution of pairs that did not fall within our selection limits, and thus identified as most likely to be chance alignments (open and filled triangles).

#### 3.2. Parallax confirmation

These pairs of *Hipparcos* stars make an excellent case study for our wide binary search algorithm because the *Hipparcos* catalog provides accurate and independent measurements of their parallaxes, which allow us to verify if the two components indeed physically associated. Overall, we find that all

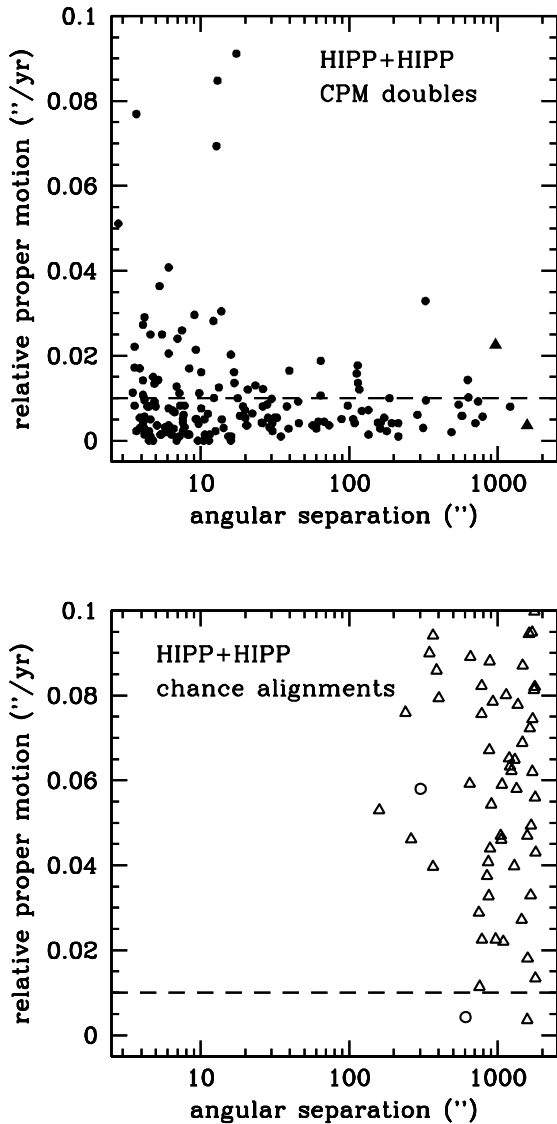


FIG. 3.— Distribution in angular separation  $\Delta\theta$  and relative proper motion  $\Delta\mu$  for pairs composed of two *Hipparcos* stars. Top panel: pairs identified as wide binaries. Bottom panel: pairs identified as probable chance alignments. Circles denote the pairs initially selected as common proper motion doubles by our search algorithm. Two of these were found to have inconsistent *Hipparcos* parallaxes, and marked as chance alignments (open circles). Triangles denote the pairs initially rejected by our search algorithm. Two of the pairs were reinstated as candidate wide binaries based on the similarity of their parallax measurements (filled triangles).

except 2 of the pair have the parallax of the primary and secondary within  $2.0\sigma$  of the measurement errors. For the 2 pairs with mismatched distances, we can only conclude that they are chance alignments. These pairs are represented in Fig.3 as open circles (bottom panel).

One of the rejected pairs is formed of LSPM J0722+0849S (HIP 35756) and LSPM J0722+0854 (HIP 35750), and has an angular separation of  $302''$ . The alleged primary has a *Hipparcos* parallax  $\pi_1 = 5.9 \pm 2.1$  mas, while the secondary has  $\pi_2 = 22.4 \pm 1.6$  mas. The two parallax measurements are thus significantly different. We note that the difference in proper motion  $\Delta\mu$  is also substantial, and it is thus not a

surprise that the two should come out as chance alignments. The pair was initially selected by our algorithm is mainly because of the relatively large proper motion of the two stars ( $\approx 0.3'' \text{ yr}^{-1}$ ), which makes this alignment a rare event given the relative scarcity of stars with very large proper motions. This pair was similarly identified as a chance alignment by Allen, Poveda, & Herrera (2000).

The other rejected pair consists of LSPM J1826+0846 (HIP 90355) and LSPM J1826+0836 (HIP 90365), with an angular separation of  $608''$ . The first star has a *Hipparcos* parallax  $\pi_1 = 37.7 \pm 1.7$  mas, while the second star has a parallax  $\pi_2 = 26.3 \pm 1.1$  mas. Again, the large difference between the two values indicates that the two are physically unrelated. Here, however, it comes out more as a surprise because the two stars have proper motion vectors within only  $4 \text{ mas yr}^{-1}$  of each other. This striking alignment of both angular positions and proper motion vectors serves as a good warning about the possibility of having physically unrelated stars come up as apparent CPM doubles.

### 3.3. Search for additional pairs

We also examined all pairs rejected in the initial cut, and with angular separations  $\Delta\theta < 2,000''$ , to see if additional CPM binaries could be recovered based on their *Hipparcos* parallaxes. This is one way to check that the algorithm does a good job at picking out most of the genuine wide binaries. An examination of the parallaxes of the primaries and secondaries in 55 pairs with  $\Delta\theta < 2000''$  (all rejected on the first pass) reveals the existence of two pairs that are indeed consistent with being CPM doubles. More specifically, the parallaxes of the individual components in each of these pairs are consistent with the two stars being at the same distance. In each of them, the parallaxes of both the primary and secondary are better than 10% accurate, and the difference between the parallax of the primary and secondary was smaller than the quoted measurement error. We have added these two pairs to our list of CPM doubles. In Fig.3, they are plotted as filled triangles. Note that both pairs have fairly small difference in their proper motion, which is also consistent with the components forming physical pairs.

One of the two very wide pairs is composed of the  $V = 6.0$  star HIP 53791 with the  $V = 10.8$  star HIP 53756 at a separation  $\Delta\theta = 968''$ . The two stars have *Hipparcos* parallaxes  $\pi = 22.0 \pm 0.8$  and  $\pi = 22.1 \pm 2.0$ , respectively. The second pair consists of the  $V = 6.9$  star HIP 75104 with the  $V = 9.0$  star HIP 75011. The very large separation between the two components ( $\Delta\theta = 1582''$ ) raises suspicion about their physical association, but the *Hipparcos* parallaxes are a near perfect match, with  $\pi = 22.7 \pm 0.8$  and  $\pi = 22.3 \pm 1.2$ . At a distance of 44 pc, the projected physical separation between the two components would be  $\sim 70,000$  AU.

It is interesting to note that the 2 genuine doubles found among the 55 pairs that were initially rejected suggest that a few percent of the pairs rejected in our search algorithm are likely to be true doubles. This emphasizes the limitations of our statistical method in making a complete identification of wide CPM doubles, especially of those with very large angular separations."

### 3.4. Complete list of wide *Hipparcos*+*Hipparcos* systems

Table 1 gives a list of the 158 doubles and 5 triples ultimately selected as wide binary systems. The table give the LSPM catalog number of the primary (column 1), the *Hip*-

*parcos* catalog number of the primary (2), its Right Ascension (3), its Declination (4), its proper motion in the direction or R.A. and in  $'' \text{yr}^{-1}$  (5), its proper motion in the direction of Decl. also in  $'' \text{yr}^{-1}$  (6), its apparent  $V$  magnitude (7), its  $V-J$  optical-to-infrared color (8), its parallax in milliarcseconds (9), the estimated parallax error in milliarcseconds (10), the angular separation between the primary and secondary in  $''$  (11), all followed by the LSPM catalog number of the secondary (12), the *Hipparcos* catalog number of the secondary (13), its Right Ascension (14), its Declination (15), its proper motion in the direction or R.A. and in  $'' \text{yr}^{-1}$  (16), its proper motion in the direction of Decl. in  $'' \text{yr}^{-1}$  (17), its apparent  $V$  magnitude (18), its  $V-J$  optical-to-infrared color (19), its parallax in milliarcseconds (20), and finally the estimated parallax error for the secondary in milliarcseconds (21). In Table 1, each of the 5 triple systems is represented by two separate (out of the possible three) pairings. The triples all consist of one short separation pair with an additional component at larger separations. The short separation pair is listed in Table 1. The large separation component is listed in a pair with the brightest component of the short separation pair. Each triple is thus referenced as one short period pair and one long period pair.

We find that of the 158 doubles and 5 triples reported here, only 80 of the doubles (and none of the triples) had been previously reported in GC04. A little more than half the systems in our list are thus “new” CPM systems.

#### 4. WIDE BINARIES WHERE ONLY THE PRIMARY IS A *HIPPARCOS* STAR

##### 4.1. Identification

Using again the method described in §2, we searched the LSPM-north catalog for CPM multiples consisting of one *Hipparcos* star with one or more non-*Hipparcos* companions. We identified a total of 347 CPM doubles, 10 triples, and 1 quadruple system. All systems are listed in Table 2. Figure 4 shows the distribution in  $\Delta\theta, \Delta\mu$  for all the pairs found with separations  $3'' < \Delta\theta < 1,500''$ . Pairs selected as probable CPM doubles are displayed on the top panel, while the rejected pairs (probable chance alignments) are shown in the bottom panel.

Note that several pairs with separations  $\Delta\theta < 100''$  are found to have relative proper motions  $\Delta\mu = 0$ ; this is an artifact of the LSPM-north catalog. The proper motions listed in the LSPM-north are based on proper motion measurements of the stars in the Digitized Sky Survey (DSS), derived with the SUPERBLINK software (Lépine & Shara 2005). The DSS images are scans from the POSS-I and POSS-II photographic plates. Companions of *Hipparcos* stars with separations  $\lesssim 20''$  are generally found within the extended wings of the bright stars, which are deeply saturated on the DSS images. In those instances SUPERBLINK identifies the mingled pair as a single extended, moving object, and calculates a proper motion for the pair only. The individual components are usually recovered by visual inspection of either the DSS scans or 2MASS charts. But even though the stars appear on separate entries in the LSPM-north, the catalog lists the SUPERBLINK-calculated proper motion of the *pair* for both the primary and secondary. Since their proper motions are listed as exactly the same, one gets  $\Delta\mu = 0$  for those pairs. We have verified each of those pairs individually using our SUPERBLINK-generated finding charts, and confirmed that in every case the two stars do indeed have very similar proper

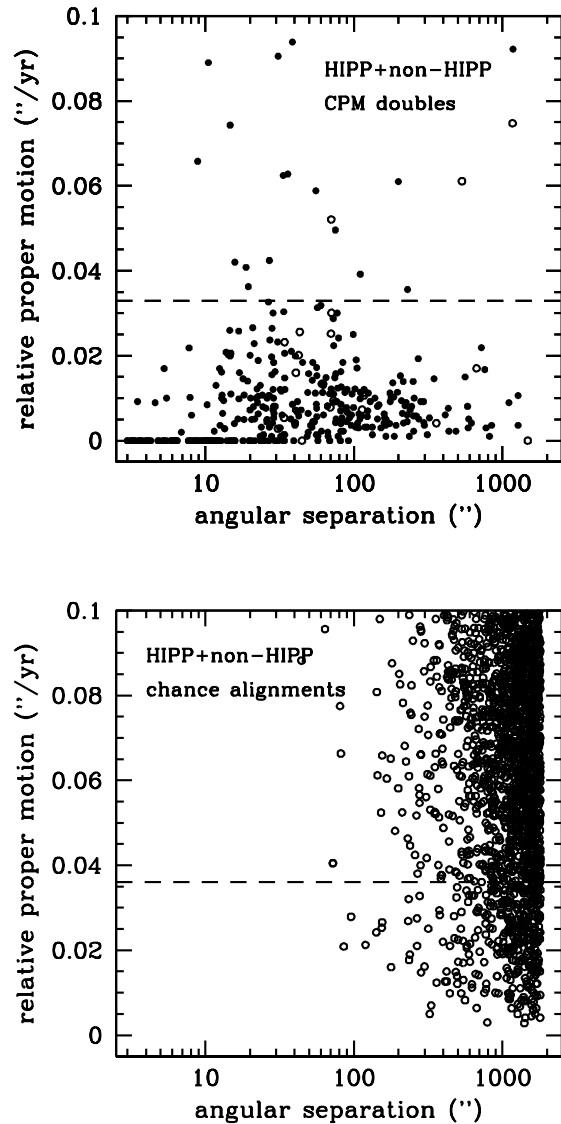


FIG. 4.— Distribution in angular separation  $\Delta\theta$  and relative proper motion  $\Delta\mu$  for pairs for which only the primary is a *Hipparcos* star. Top panel: pairs identified as probable wide binaries by our search algorithm. Open symbols denote doubtful pairs, in which the photometric distance of the secondary are inconsistent with a physical association. Bottom panel: pairs rejected by the algorithm and most likely to be chance alignments.

motions, so it is very unlikely that any of those pairs could be chance alignments, and their initial identification as CPM doubles is valid.

##### 4.2. Photometric distance verification

Because we lack parallax measurements for the non-*Hipparcos* secondaries, it is not possible to verify the binary status of these pairs by direct comparison of their measured distances, as we did in §3. Another test, however, is to check that the color and magnitude of the secondary is at least consistent with the star being at the same distance from the Sun as its primary. This is equivalent to comparing the parallax distance of the primary with the photometric distance of the secondary. We can plot the secondary star in a color-magnitude

diagram, using the parallax of the *primary star* to calculate its alleged absolute magnitude. If the two stars are indeed physically associated, then the secondary should fall on the standard main sequence, or on the white dwarf cooling sequence. If the secondary stars doesn't fall where it should be on the color magnitude diagram, then either the secondary is really not at the same distance from the Sun as the primary, and the pair is a chance alignment, or the secondary star has an absolute magnitude which doesn't fit with the standard stellar loci.

Color magnitude diagrams for the primaries and secondaries are displayed in Figure 5. In these diagrams, the absolute magnitudes of both the primaries and secondaries are calculated using the parallaxes of the *Hipparcos* primary stars. The diagrams are built in the (V,V-J) system of visual magnitude and optical-to-infrared color, a system most useful for displaying the cool end of the main sequence and perhaps the most appropriate for our sample of secondary stars, which is dominated by cool red dwarfs. Secondaries found in the immediate vicinity of bright *Hipparcos* stars often suffer from large measurement errors in their optical V magnitudes, which are derived from POSS plate measurements. For that reason, we separate the secondaries into two distinct groups, those with angular separations  $\Delta\theta < 30''$  and those with  $\Delta\theta > 30''$ . The color-magnitude test is expected to fail for many of the closer pairs because of possible large errors in their estimated V magnitude. Fortunately, pairs with small separations have a very low probability of being chance alignments, so it is safe to assume that they are physically associated, in any case.

Figure 5 shows color-magnitude diagrams for the primaries (top), the close  $\Delta\theta < 30''$  secondaries (middle), and the wide  $\Delta\theta > 30''$  secondaries (bottom). The figure also plots in diagrams in two separate columns, comparing the pairs with *Hipparcos* secondaries from §2 (left) with the pairs with non-*Hipparcos* secondaries (right). Overall, we find that the majority of the secondaries fall close to either the main sequence or the white dwarf cooling sequence. A pair of dotted lines delimitates a the region where stars are within 1.5 mag of the standard main sequence (upper right in the diagram) as determined from a fit of nearby stars with known trigonometric parallaxes (Lépine 2005). A second pair of lines identifies the region within 1.5 mag of the standard white dwarf sequence based on the distribution of nearby white dwarfs with known trigonometric parallaxes (Lépine 2006, in preparation).

Secondaries with  $\Delta\theta < 30''$  are found to exhibit a significantly larger dispersion about the main sequence than the pairs with  $\Delta\theta > 30''$ . For the pairs with *Hipparcos* secondaries, the  $\Delta\theta > 30''$  companions have a mean position of only 0.01 mag above the main sequence with a  $1\sigma$  dispersion of 0.39 mag; the only clear outlier (at  $M_V=1.27$ ,  $V-J=1.97$ ) is the star HIP 64522 = HD 115061, a known giant star. The *Hipparcos* secondaries with  $\Delta\theta < 30''$ , one the other hand, have many more clear outliers. If we disregard all the secondaries that are off the main sequence by more than 3 magnitudes, we still find that the companions lie on average 0.42 mag above the main sequence, with a dispersion of 0.95 mag. This larger dispersion suggests that the magnitudes and colors of the closer companions carry large uncertainties, and the 0.42 mag offset even suggests possible systematic errors. Likewise the magnitudes and colors of the non-*Hipparcos* secondaries are clearly more scattered around the main sequence for companions with ( $\Delta\theta < 30''$ ). Even if we exclude the 3-magnitude outliers, we find that the close secondaries

are on average 0.11 mag below the main sequence with a dispersion of 1.33 mag. Companions with  $\Delta\theta > 30''$  have a mean offset of 0.05 mag with a significantly smaller dispersion of only 0.45 mag. We conclude that the colors and magnitudes of the short separation pairs ( $\Delta\theta < 30''$ ) are not reliable enough to be useful for a photometric distance comparison. For the large separation pairs ( $\Delta\theta > 30''$ ), however, the colors and magnitudes are accurate enough to use the photometric distance of the secondary as a confirmation that the two components are physically related.

It is clear from Fig.5 that several of the wide secondaries do fail the test. The lower-right panel shows several secondaries that are outliers of both the red dwarf and white dwarf sequences. We identify a total of 20 pairs with mismatched companions; these are listed separately in Table 3. Nine of these uncertain secondaries are found lying  $\approx 2$  magnitudes above the standard main sequence. One possible explanation is that these secondaries are actually foreground red dwarfs in chance alignments with background *Hipparcos* stars. Another possibility is that these secondaries are actually unresolved double stars (in which case these would really be triple systems). An unresolved pair of stars with components of similar color and absolute magnitude will appear 0.75 mag brighter than a single star of the same type. Reducing the absolute magnitudes of those “overluminous” secondaries by 0.75 mag, to account for unresolved companions, would bring them back within range of the standard main sequence. The binary status of these stars should be verified through either high angular resolution imaging (e.g. Beuzit *et al.* 2004; Law *et al.* 2006) or radial velocity monitoring (e.g. Delfosse *et al.* 1999).

The remaining 11 “uncertain” companions are found lying between the main sequence and white dwarf cooling sequence. The simplest interpretation is that these stars are background red dwarfs in chance alignments with foreground *Hipparcos* stars. They could also be foreground white dwarfs in chance alignments with background *Hipparcos* stars. Another possibility, however, is that these secondaries are red subdwarfs. Red subdwarfs are the metal-poor counterparts of the main sequence red dwarfs; in the color magnitude diagram, the subdwarf sequence is found to the left (blueward) of the main sequence (Monet 1992; Fuchs & Jahreiss 1998). This is because lower metallicities result in lower atomic and molecular opacities in the optical bands, shifting the spectral energy distribution to the blue (Allard & Hauschildt 1995). In the ( $M_V, V-J$ ) color-magnitude diagram, red subdwarfs are expected to fall between the main sequence and the white dwarf sequence.

A simple kinematic test can be applied to check if a star is a good subdwarf candidate. In the Solar neighborhood, subdwarfs generally exist as high-velocity stars. This is because local metal-poor stars are usually members of the Galactic halo or thick disk (Chiba & Beers 2000). In Figure 6, we plot the projected, transverse velocities  $V_T$  of our CPM doubles, against their angular separation  $\Delta\theta$ . The top panel shows pairs which have secondaries that consistently fall on the main sequence when placed at the primary's distance (see Fig.5). The bottom panel shows the uncertain pairs, including those for which the secondaries are suspected to be subdwarfs (using the same symbols as in Fig.5).

We find only one pair with a transverse velocity which clearly associate it with the halo population. This is the pair whose primary is the star HIP 35756 (G 89-14) a known spectroscopic double (Latham *et al.* 2006). Although its parallax



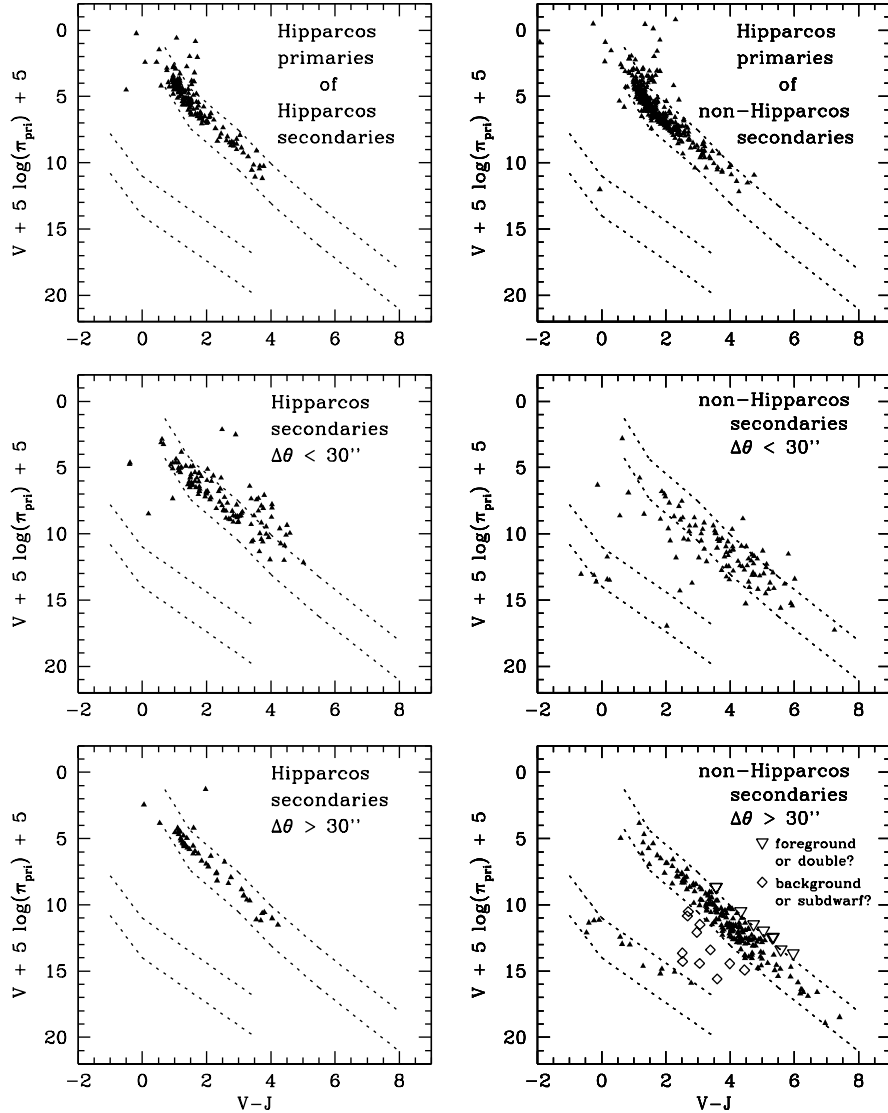


FIG. 5.— Color-magnitude diagrams of the components of the pairs identified in our search for wide binaries. Left panels: diagrams for the pairs where both components are *Hipparcos* stars. Right panels: diagrams for the pairs where only the primary is a *Hipparcos* star. In all diagrams, the absolute magnitude is calculated using the parallax of the primary. Primaries are shown in the top row, the middle row shows the secondaries found within  $30''$  of their primaries, and the bottom row the secondaries found beyond  $30''$  of their primaries. In the tight pairs, the secondaries are susceptible to large magnitude errors because of the neighboring presence of the very bright primaries. Their location on the color-magnitude diagrams are inconclusive. In the wide pairs, the magnitudes and colors of the secondaries are more reliable, and they are expected to be found within the locus of main sequence stars or white dwarfs. Secondaries that fail this test (open symbols) may be foreground or background stars, unresolved doubles, or subdwarfs.

is fairly uncertain ( $\pi = 5.9 \pm 2.1 \text{ mas}$ ), G 89-14 has long been known to be a metal-poor subdwarf, with  $\log(\text{Fe}/\text{H}) \approx -1.6$  (e.g. Schuster & Nissen 1989). The relatively small angular separation to the secondary ( $34''$ ) further argues in favor of this pair being a physical double (or rather triple, since the *Hipparcos* primary is itself an unresolved double). Indeed, this CPM multiple had already been identified as a physical pair by Allen, Poveda, & Herrera (2000), in their search for wide binaries among known metal poor stars.

The primaries of the remaining 10 objects, on the other hand, have kinematics more consistent with the disk population, which makes the alleged secondaries unlikely to be subdwarfs. For the 4 pairs with the largest separations  $\Delta\theta > 300''$ , a good case can be made that they are most likely to be chance alignments. The situation is not so clear for the 6 other pairs, which have  $30'' < \Delta\theta < 75''$ : the proximity of the compo-

nents argues against simple chance alignments. Either these stars have large errors in their magnitudes, or they are most likely to be subdwarfs. The subdwarf status of the alleged CPM companions should be checked more directly through spectroscopic measurements. Metallicity effects can be diagnosed in optical spectra from the ratio of the TiO and CaH bandstrengths (Gizis 1997; Lépine, Rich, & Shara 2003). If both the primary and secondary have spectra consistent with a low metallicity object (i.e. if they are both spectroscopic subdwarfs) then they are most likely to be actual physical doubles. If on the other hand, the stars are both found to be regular dwarfs, then the pair must be a chance alignment. If one component is found to be a dwarf and the other a subdwarf, then it would also strongly suggest that the pair is a chance alignment, since one would expect CPM doubles to have similar chemical compositions.

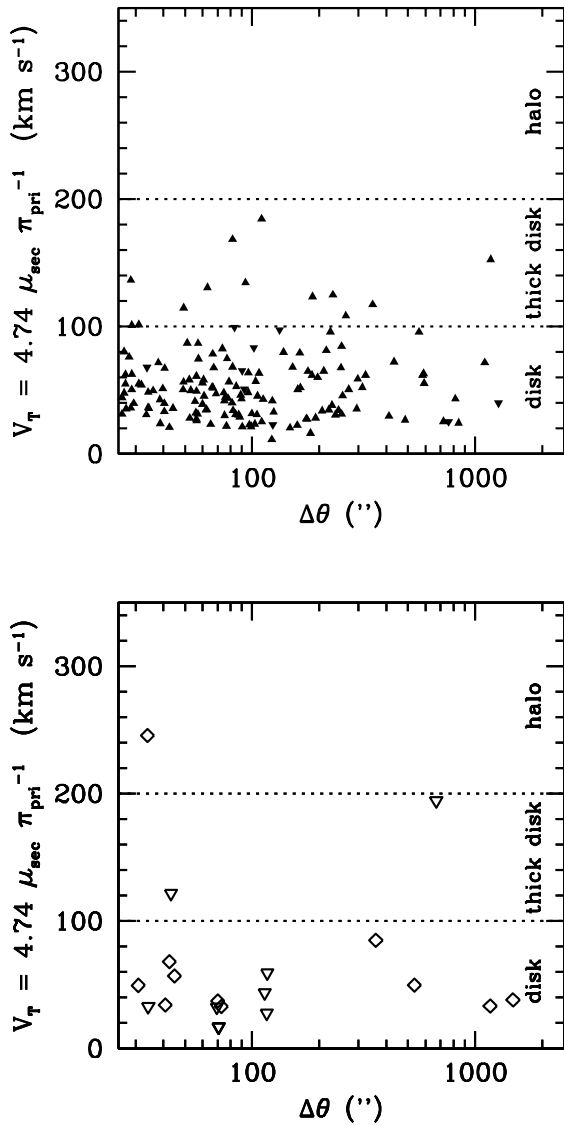


FIG. 6.— Projected, transverse velocities  $V_T$  as a function of angular separation  $\Delta\theta$  for pairs in which only the primary is a *Hipparcos* star. Top panel: pairs with matching photometric distances. Bottom panel: pairs where the secondaries have inconsistent photometric distances; symbols are the same as in Fig. 5. Of the 13 pairs that could be hosting a subdwarf secondary, only one has kinematics consistent with the standard subdwarf population (thick disk/halo). This suggests that the remaining 12 pairs are most likely to be chance alignments.

#### 4.3. Overlooked pairs and survey completeness

Given the angular separation limits of our search algorithm, we do expect to be overlooking genuine wide binaries with very large angular separations. The range of our search actually depends on the proper motion of the pair. For instance, pairs with a mean proper motion  $\mu = 0.15'' \text{ yr}^{-1}$  and proper motion differences  $\Delta\mu = 10 \text{ mas yr}^{-1}$  will not make it into the sample if  $\Delta\theta > 100''$ . Proper motions in the LSPM-north catalog have a mean error of  $8 \text{ mas yr}^{-1}$ , which at first guess suggests typical proper motion differences  $\Delta\mu \approx 11.3 \text{ mas yr}^{-1}$ , for CPM binaries. The actual errors in  $\Delta\mu$  are probably somewhat smaller, because part of the  $8 \text{ mas yr}^{-1}$  proper motion er-

rors in the LSPM-north are due to systematic errors, which affect both stars in a CPM pair equally, and these systematic errors subtract out in  $\Delta\mu$ . In any case, we conservatively adopt  $11.3 \text{ mas yr}^{-1}$  as the mean error in  $\Delta\mu$ , and place a  $3\text{-}\sigma$  limit at  $\Delta\mu = 34 \text{ mas yr}^{-1}$ . Since this is larger than our adopted detection limits at large separations, we conclude that it is likely that at least a few genuine pairs have been rejected by our search algorithm.

A look at Fig. 4 (bottom panel) shows a handful of pairs with angular separations  $\Delta\theta < 300''$  and relative proper motions  $\Delta\mu < 33 \text{ mas yr}^{-1}$  (dashed line) that were not selected by our algorithm. While these pairs still have a fairly high probability of being chance alignments, we cannot exclude the possibility that a significant fraction of them are wide binaries. Assuming that all the pairs with  $\Delta\mu < 33 \text{ mas yr}^{-1}$  are actually wide binaries, we calculate that these would represent only 5% of the total pairs found. Hence we are confident that our census must be at least 95% complete up to  $\Delta\theta = 300''$ . Beyond that limit, the completeness of our survey probably falls as the angular separation increases.

#### 4.4. Complete list of wide binaries with a *Hipparcos* primary

Table 3 gives a list of the 347 doubles, 10 triples, and 1 quadruple ultimately selected as wide binary systems. The table give the LSPM catalog number of the primary (column 1), the *Hipparcos* catalog number of the primary (2), its Right Ascension (3), its Declination (4), its proper motion in the direction or R.A. and in  $'' \text{ yr}^{-1}$  (5), its proper motion in the direction of Decl. also in  $'' \text{ yr}^{-1}$  (6), its apparent  $V$  magnitude (7), its  $V-J$  optical-to-infrared color (8), its parallax in milliarcseconds (9), the estimated parallax error in milliarcseconds (10), the angular separation between the primary and secondary in  $''$  (11), all followed by the LSPM catalog number of the secondary (12), its Right Ascension (13), its Declination (14), its proper motion in the direction or R.A. and in  $'' \text{ yr}^{-1}$  (15), its proper motion in the direction of Decl. in  $'' \text{ yr}^{-1}$  (16), its apparent  $V$  magnitude (17), and its  $V-J$  optical-to-infrared color (18). As in Table 1, the triple systems are represented by two separate (out of the possible three) pairings. The quadruple system is represented by 3 pairings. A flag in column 20 identifies the triples and quadruple.

Of the 400 pairings with non-*Hipparcos* secondaries, 208 are listed in GC04; these stars are indicated with a “GC” flag in Table 3. Some 134 of these were also listed in Luyten’s LDS catalog. We find 26 additional pairs not listed in GC04, but listed in the LDS catalog. The remaining 130 pairs are new wide binary systems, reported here for the first time. We note that out of the 156 pairs that are not listed in GC04, 145 are pairs for which the primary and/or secondary was not listed in the rNLTT catalog, which explains their absence from the GC04 list. For the 22 systems whose primaries and secondaries are both listed in the rNLTT as well as in the LSPM-north, we found one (with HIP 102040 as the primary) that has a proper motion difference  $\Delta\mu = 20.7 \text{ mas yr}^{-1}$  in the rNLTT, which places it just outside of the selection range used in GC04 ( $\Delta\mu < 20.0$ ). The LSPM-north proper motions yield a  $\Delta\mu = 11.2 \text{ mas yr}^{-1}$  for that pair, well inside our own detection range. The other 21 pairs, however, have  $\Delta\theta$  and  $\Delta\mu$  within the selection limits of GC04, and it remains unclear why they were not included in their list.

Within the limits of our search area (the northern sky), we found only 4 pairs in the GC04 list that were not picked up by our search algorithm. These 4 pairs have HIP 45488, HIP

51547, HIP 53008, and HIP 64386 as their primary stars. Their alleged CPM companions are relatively distant, with angular separations of  $444''$ ,  $142''$ ,  $178''$ , and  $453''$  respectively. We found differences in proper motion of  $21 \text{ mas yr}^{-1}$ ,  $24 \text{ mas yr}^{-1}$ ,  $16 \text{ mas yr}^{-1}$ , and  $79 \text{ mas yr}^{-1}$ , respectively, for these pairs; these fairly large differences, and the large angular separations, explains why they fell outside our selection zone. It is possible that some of these pairs, and other pairs rejected in our algorithm, might be genuine physical doubles, particularly those that just barely fell off the selection limit.

Overall, we find that our own census recovers essentially all the GC04 pairs, and adds a significant number of new objects. The improvement clearly comes from the use of the more complete LSPM-north catalog. Given the very high estimated completeness of the LSPM-north, we are confident that we have now identified virtually *all* existing companions of *Hipparcos* stars within a relatively large range of angular separations, and down to an apparent magnitude  $V = 19$ .

## 5. ANALYSIS OF THE WIDE BINARY CENSUS

### 5.1. Distances and orbital separations

We have determined in §4.3 that our census is statistically (> 95%) complete up to angular separations  $\Delta\theta = 300''$ . The survey also has a limit at small angular separations. The large apparent magnitude of the *Hipparcos* primaries and their deep saturation on photographic survey plates hampers our detection of companions with small angular separations. Since the LSPM-north is based on analyses of Digitized Sky Survey scans of POSS-I and POSS-II, this is a severe limitation because *Hipparcos* stars are deeply saturated on POSS-I plates. For pairs where only one component is a *Hipparcos* star, we should be able to see companions only for angular separations  $\Delta\theta \gtrsim 10''$ . Some companions in the LSPM-north have been resolved from 2MASS images, but this is possible only for relatively bright companions, in any case much brighter than the  $V = 19$  catalog limit.

Pairs for which both components are *Hipparcos* stars are not limited in the same way, because the LSPM-north uses the *Hipparcos* catalog itself as input for the brighter stars. All pairs with  $\Delta\theta \gtrsim 3''$  should be resolved in the *Hipparcos* catalog. We can thus use the statistically complete distribution in angular separations of the *Hipparcos*+*Hipparcos* pairs to estimate the incompleteness of our census for pairs with faint secondaries.

Figure 7 plots the projected orbital separations  $s = \pi^{-1} \Delta\theta$  of the pairs as a function of their distance  $d = \pi^{-1}$  (estimated from the *Hipparcos* parallaxes  $\pi$ ). Note that our systems tend to be relatively nearby, with most of the pairs lying at distances 20-100 parsec. The fact that fewer pairs are detected at larger distances is the result of proper motion selection effects. Because of the lower limit  $\mu > 0.15'' \text{ yr}^{-1}$  of the LSPM-north, stars with low transverse velocities are increasingly left out of the sample at larger distances (Lépine 2005). The number of detected systems hence reaches a maximum around  $d \approx 40$  pc.

What is also apparent in Fig.7 is the dominance of pairs  $\Delta\theta < 20''$  in the HIP+HIP systems. In contrast, pairs for which only the primary is a *Hipparcos* star, are mostly found with  $\Delta\theta > 20''$ . Our census of systems with faint secondaries is thus clearly undersampled in pairs with  $\Delta\theta < 20''$ . This is largely consistent with our prediction that secondaries with small angular separations would be lost in the glare of their bright primaries. We conclude that our census is thus statisti-

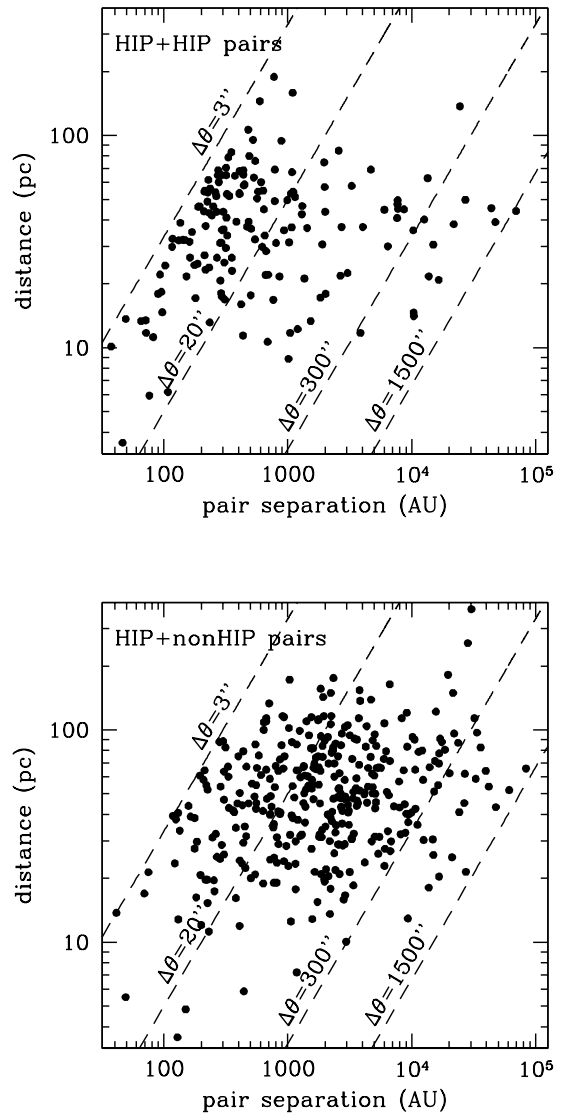


FIG. 7.— Calculated projected physical separations of the wide binaries identified in our survey (in Astronomical Units). The census is much more complete at small angular separations for pairs of *Hipparcos* stars (top). For non-*Hipparcos* companions, the census appears to be complete only beyond  $\Delta\theta > 20''$ . Pairs are however detected up to  $\Delta\theta \approx 1,500''$ , which gives an excellent coverage of the 1,000-10,000 AU separation range.

cally complete only over the range  $20'' < \Delta\theta < 300''$ .

While our census spans only 1.3 orders of magnitude in  $\Delta\theta$ , we are actually sensitive to a larger range of projected orbital separations  $s$  because our sample covers systems over a relatively large range of distances. Since our pairs are found in a range of distances  $15 \text{ pc} < d < 100 \text{ pc}$ , our effective sampling range for wide companions is between 300 AU and 30,000 AU. It is worth noting that this extends beyond the canonical upper limit  $s < 0.1 \text{ pc}$  ( $= 20,000 \text{ AU}$ ) for wide binary systems (Close, Richer, & Crabtree 1990). Our sample actually suggests the existence of wide binaries with  $s > 0.1 \text{ pc}$ . Our widest binary system is the pair composed of HIP 64157 and the faint high proper motion star LSPM J1308+3332 ( $= \text{NLTT } 33016$ ), which have an angular separation  $\Delta\theta = 1273.7''$  and

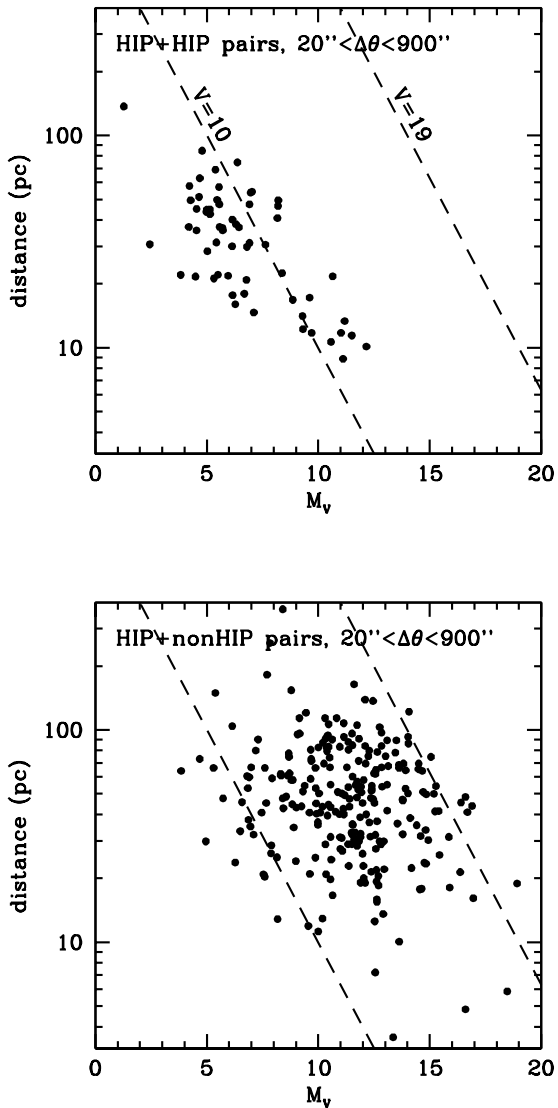


FIG. 8.— Absolute magnitude of the secondaries plotted against the distance of the common proper motion systems. Few of the *Hipparcos* secondaries are found with apparent magnitude  $V > 10$  due to the increased incompleteness in the *Hipparcos* catalog (top panel). Many more secondaries are found with the LSPM-north (bottom), which is statistically complete down to  $V = 19$ . One can see the turnover in the luminosity function beyond  $M_V = 14$ , which is similar to the turnover in the luminosity function of field single stars.

are located at a distance  $d \approx 65$  pc, which yields an orbital separation  $s \approx 83,000$  AU. Note that the pair has a relatively large transverse velocity  $V_{tran} \approx 70$  km  $s^{-1}$ , which rules out the alternate interpretation that the two stars are co-moving members of a young association.

### 5.2. Absolute magnitudes of the secondaries

Figure 8 shows the distribution in absolute magnitudes  $M_V$  and distances of the CPM secondaries, for pairs with separations  $20'' < \Delta\theta < 900''$ . In this range of angular separations, our census should be nearly complete down to the limiting magnitude of the LSPM-north catalog i.e.  $V = 19$ . We show distinct plots for *Hipparcos* secondaries (top) and non-*Hipparcos* secondaries (bottom). The secondaries are clearly

dominated by stars with  $10 < M_V < 15$ , in other words by M dwarfs. Since most of the *Hipparcos* primaries are G dwarfs, with  $5 < M_V < 8$ , it is clear that there is no general tendency for the secondaries to be of similar masses as their primaries. The secondaries, in fact, look like they could have been drawn from the field population of single stars (see however §5.3 below).

The magnitude limit of the LSPM-north catalog yields a limiting absolute magnitude which is dependent on the distance of the pair. The majority of our pairs are relatively close; if we restrict our sample to objects within  $d < 100$  pc, then our census of faint secondaries should be complete down to  $M_V = 14$ . This happens to be just beyond the peak in the luminosity function of low-mass red dwarfs (Reid, Gizis, & Hawley 2002). Assuming the luminosity function of the secondaries to be roughly similar to that of field stars, then our census should be missing only a relatively small fraction of the Hydrogen-burning secondaries. In any case, our detection of several very nearby ( $d < 20$  pc) secondaries with  $M_V > 15$  suggests that several very-low mass companions remain to be discovered at larger distances. To be detected, these will require catalogs of high proper motion stars with significantly fainter magnitude limits.

### 5.3. Luminosity function of the secondaries

A close examination of the distribution in the absolute magnitude of the CPM secondaries shows a deficit of low-luminosity objects ( $M_V > 9$ ) compared with the field luminosity function. Figure 9 shows the  $M_V$  distribution for the primaries and secondaries in our sample. We use a Monte-Carlo simulation to predict the magnitude distribution of the secondaries, using the assumption that both components are drawn independently from the field luminosity function. We adopt the luminosity function of main sequence stars in the Solar Neighborhood estimated by (Reid, Gizis, & Hawley 2002); the additional contribution of the white dwarfs can be neglected, since they account for less than 5% of the secondaries. As shown in Fig.9, the distribution observed for the secondaries is significantly different from the predicted one. If we adjust the simulations to match the numbers of bright ( $M_V < 8$ ) secondaries, we find only  $\approx 60\%$  of objects in the  $9 < M_V < 14$  range predicted by the model. Since our census is demonstrably complete at  $d < 100$  pc down to  $M_V = 14$ , the difference is significant, and rules out the idea that the luminosity function of the secondaries is comparable to the field luminosity function.

Since the absolute magnitude of main sequence stars is correlated with mass, the dearth in low-luminosity objects indicates that low-mass stars are less likely to be found as CPM secondaries than they are in the field population. One simple interpretation is that the formation mechanisms for wide binaries are biased against secondaries of very low mass or, equivalently, that they are biased in favor of high-mass secondaries. Another possible interpretation is that wide binaries are formed initially with both components drawn from the same mass function, but that gravitational interactions with the environment disrupt a number of systems over time, in events that favor the disruption of systems with low-mass secondaries.

In fact, if we assume that both components in wide binaries initially follow the field luminosity function, then the ratio between the observed (or “current”) and predicted (“initial”) luminosity function (Fig.9) shows a trend that suggest that the lower the mass of the secondary, the higher the probability for

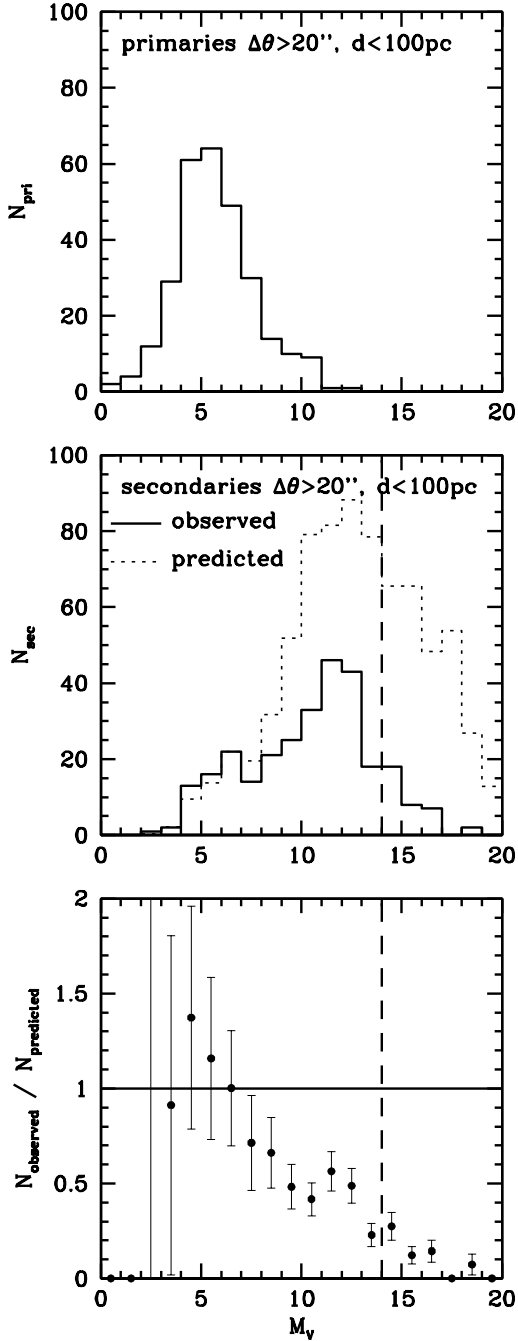


FIG. 9.— Distribution in absolute magnitude  $M_V$  for the primaries (top) and secondaries (center) in our sample of wide binaries. The observed luminosity function of the secondaries is found to be significantly deficient in faint stars ( $M_V > 9$ ) compared to the distribution predicted if both components are drawn from the field luminosity function of (Reid, Gizis, & Hawley 2002). The observed distribution contains only  $\approx 60\%$  of the predicted number of faint secondaries. The dashed line shows the completeness limit of our sample ( $M_V < 14$ ).

the wide system to have been disrupted over time. Should this interpretation be correct, then one should expect to find very few faint companions of *Hipparcos* stars with absolute magnitudes  $M_V > 14$ . This would imply that our sample is already nearly complete for wide Hydrogen-burning companions, and that very few fainter companions should be found.

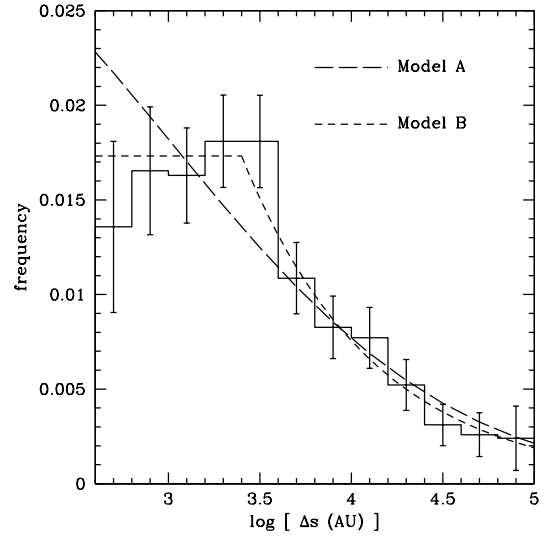


FIG. 10.— The frequency of wide binary systems in the Solar Neighborhood, as estimated from our sample of *Hipparcos* stars with distant common proper motion companions. The frequency is calculated for each bin, which samples the projected orbital separation  $s$  in steps of 0.2. Two possible models are shown: model A is the tail of an gaussian, model B follows Öpik’s law ( $f(s) \sim \Delta s^{-1}$  ds) up to 2,500 AU, then breaks down to a power law  $f(s) \sim \Delta s^{-1.6}$ .

#### 5.4. Observed frequency of wide binary systems

From our statistically complete sample of CPM pairs with *Hipparcos* primaries, we can now estimate the multiplicity fraction of wide binary systems in the Solar Neighborhood. We have determined that our northern-sky census was statistically complete for systems within 100 pc and proper motion  $\mu > 0.15'' \text{ yr}^{-1}$ , and for CPM companions with luminosities  $M_V < 14$ . We estimate the multiplicity fraction by comparing the number of wide binaries found in our survey to the total number of *Hipparcos* stars in the same range of position, distance, and proper motion. A search of the *Hipparcos* catalog finds a total of 3,041 stars north of the celestial equator with proper motion  $\mu > 0.15''$ , parallaxes  $\pi > 10$  mas, and a parallax accuracy of better than 10%.

We calculate the number density of wide binaries as a function of the logarithm of the *projected*, orbital separation between the pairs  $\log s$ , with  $s$  expressed in AU. Note that  $s = S \sin(i)$ , where  $S$  is the actual orbital separation between the components and  $i$  the orbital inclination. While  $S$  is the physically meaningful quantity, we only have  $s$  as the observable. We separate our sample into bins of 0.2 in  $\log s$ . We calculate the multiplicity fraction for each bin by taking the ratio of wide binaries found in that bin to the total number of *Hipparcos* stars which satisfy the distance detection limits for that bin, based on a range of angular separations  $20'' < \Delta\theta < 900''$ . For instance, the  $\log s = 3.1$  bin can only comprise systems with distances between 1.4 pc and 62.9 pc (see Fig 7). The resulting wide binary frequency distribution is shown in Figure 10. Our results indicate that at least  $9.1 \pm 1.6\%$  of all stellar systems in the Solar Neighborhood consist of wide binaries/multiples with separations  $s > 1,000$  AU. More specifically, this conclusion is valid for systems in which the primary is a typical, nearby *Hipparcos* star, i.e. the primary is a G dwarf with absolute magnitude  $4 \lesssim M_V \lesssim 7$ .

We try to fit the observed distribution of orbital separation with two different models previously used in the literature. First we try a model of the form used by Duquennoy & Mayor

(1992), which modelizes the distribution over the logarithm of orbital periods  $\log P$  with a Gaussian:

$$f_P(\log P) = F_{\text{mult}} \pi^{1/2} \sigma_P \exp\left[-\frac{(\log P - P_0)^2}{2\sigma_P^2}\right], \quad (9)$$

with  $P_0 = 4.8$ ,  $\sigma_P = 2.3$ ,  $\pi = 3.141592\dots$ , and where  $F_{\text{mult}}$  is the total multiplicity fraction, i.e.  $F_{\text{mult}} = \int_{-\infty}^{\infty} f_P(P) dP$ . For the systems considered in this paper, in which the primary stars are mostly solar-type objects with masses  $M_* \sim 1M_\odot$ , we calculate the following statistical relationship between the period  $P$  and projected separation  $s$ :

$$2 \log P \simeq 3 \log s + 5, \quad (10)$$

where  $P$  is expressed in years and  $s$  in AU. We then have:

$$f_s(\log s) = F_{\text{mult}} \pi^{1/2} \sigma_P \exp\left[-\frac{(1.5 \log s + 2.5 - P_0)^2}{2\sigma_P^2}\right]. \quad (11)$$

Our attempt to fit this form to the observed distribution of projected separations is shown in Fig.10 (Model A). Our best fit does not reproduce well the form of the distribution, and predicts more objects at small separations than are actually observed. In fact, our best fit model suggests a total multiplicity fraction  $F_{\text{mult}} = 0.75$ , which is much larger than the total binary fraction estimated by Duquennoy & Mayor (1992). We take this as evidence that this particular form is inadequate in the range of orbital separations under consideration.

Our second attempt to modelize the distribution of orbital separations uses a power-law of the form:

$$f_s(s) \sim s^{-l}. \quad (12)$$

Given that the mean projected separation in a sample of systems with random orbital plane orientations is  $s \simeq 0.78S$ , then statistically the distribution in projected separations  $s$  also follows:

$$f_s(s) \sim s^{-l}. \quad (13)$$

If we plot the distribution along  $\log s$  we have:

$$f_s(\log s) \sim 10^{(1-l)\log s}. \quad (14)$$

The specific form of the equation for which  $l = 1$  is the well-known *Öpik's law*, and yields a distribution which is uniform in  $\log s$ .

We find that our data can be consistently modeled with two distinct power-law distributions over two separate ranges of orbital separations (Fig.10, Model B). At small projected separations, our data are consistent with *Öpik's law*, but only up to a separation  $s \sim 3,000$  AU. Beyond that limit, the distribution shows a sudden break, and can best be fitted with a  $l = 1.6$  power index. The latter is consistent with the trends observed by Chanamé & Gould (2004) for both their disk and halo samples. The flattening of the distribution below  $s \sim 3,000$  AU, which is also hinted at in the CG04 data, is not much of a surprise since the  $l = 1.6$  power law cannot possibly extend to much smaller orbital separations or the multiplicity fraction might take unphysical values. An extrapolation to  $S = 1.4$  ( $s = 25$  AU), for instance, would yield a total binary fraction larger than 1.

Perhaps the more significant result is not the flattening of the  $l = 1.6$  power law distribution toward small angular separations, but rather the observed break in *Öpik's Law* at large angular separations. If one believes that star formation processes initially yield a distribution of wide binary systems

consistent with *Öpik's Law*, then our data reveals the range of maximum extension of the law. *Öpik's Law* then probably breaks down because of the disruptive effects of the environment in which the stars are born. Disruption would most likely occur through interactions with neighboring stellar systems, perhaps in the very same cluster in which these systems are born. A much larger census of wide binary systems, which would yield a more detailed distribution of orbital separations, might shed more light on the processes at work in hampering the formation of extremely wide pairs.

## 6. CONCLUSIONS

We have used the LSPM-north catalog of stars with proper motions  $\mu > 0.15'' \text{ yr}^{-1}$  to conduct a search for common proper motion (CPM) companions of *Hipparcos* stars. Because of the large coverage (20,000 square degrees) and high completeness of the LSPM-north, we have obtained a large, *statistically complete* census of CPM companions over the range of angular separations  $20'' < \Delta\theta < 300''$ . Since the LSPM-north is statistically complete in high proper motion stars down to an apparent magnitude  $V = 19$ , our census of wide binaries is complete to a distance of 100 pc for companions with absolute magnitude  $M_V < 14$ . This high completeness yields the most thorough search for wide companions to *Hipparcos* stars conducted to date.

We find that the observed luminosity function of the faint secondaries appears to be biased against low-luminosity stars, when compared with the luminosity function of the field, single star population. Most of the *Hipparcos* primaries are F-G dwarfs with absolute magnitudes around  $M_V = 5$ . The secondaries, on the other hand, are dominated by fainter K-M dwarfs, with a range of absolute magnitude peaking at  $M_V = 12$ . While fainter, lower-mass companions clearly dominate over companions of similar masses and luminosities, one finds only half the number of faint secondaries as one would expect if both primaries and secondaries were drawn from the field luminosity function. The bias against low-mass secondaries also appears to get more severe at lower secondary masses.

We further observe a distribution in the projected separations  $s$  which is consistent with *Öpik's law* ( $f(s)ds \sim s^{-1} ds$ ) for systems with orbital separations up to  $\approx 3,500$  AU. Beyond that range, the frequency of wide binaries decreases according to a power law  $f(s)ds \sim s^{-1.6} ds$ . Our data thus provides clear evidence for a break in *Öpik's law* at large angular separations, and we suggest that the break occurs as interactions between neighboring systems either prevents the formation of very wide binary systems or tends to disrupt them after they are formed.

Measurements of the distribution of orbital separations remain relatively crude. A more detailed analysis of the binary frequency, which holds the promise to provide stringent constraints on multiple star formation models, will require much larger samples of CPM pairs. At this time, we plan to first expand our census to the southern hemisphere using the upcoming LSPM-south catalog (Lépine & Shara, in preparation) which will be the analog of the LSPM-north for the southern declinations. This will double our census CPM pairs. The census of wide binaries should also be expanded further by extending the search to smaller proper motion regimes. Such a survey of pairs of stars with low proper motions has recently been demonstrated by Greaves (2004), who identified 705 wide binaries among stars with proper motions ( $\mu < 0.2''$

$\text{yr}^{-1}$ ) based on an analysis of the UCAC2 astrometric catalog. The *Hipparcos* catalog has 16,753 objects within 100 parsecs and parallaxes better than 10%. However, only 6,202 of these have proper motions  $\mu > 0.15''\text{yr}^{-1}$ , the current range of our proper motion survey. However, 13,368 of these nearby *Hipparcos* stars have proper motion  $\mu > 0.05''\text{yr}^{-1}$ , so a catalog of stars with  $\mu > 0.05''\text{yr}^{-1}$  would potentially double the census of wide binaries. The census could further be expanded by investigating *Hipparcos* stars at larger recorded distances, adding up to 10,000 targets in the 100-200pc range.

It would also be desirable to break the low angular separation limit  $\Delta\theta > 20''$  of the photographic plate-based surveys. A look at Fig.7 is highly suggestive of the existence of

significant numbers of faint companions with small angular separations. With CCD imaging and adaptive optics systems, it should be possible to perform a complete census of CPM companions of *Hipparcos* stars down to angular separations of a fraction of an arcsecond. This would be particularly useful in extending the census to pairs with smaller orbital separations ( $s < 1,000$  AU) and verify whether this regime can be consistently modeled with *Öpik's Law*.

#### Acknowledgments

SL gratefully acknowledges support from Hilary Lipsitz, and from the American Museum of Natural History.

#### REFERENCES

- Abt, H. A. 1983, *ARA&A*, 21, 343  
 Allard, F., & Hauschildt, P. H. 1995, *ApJ*445, 433  
 Allen, C., Poveda, A., & Herrera, M. A. 2000, *A&A*, 356, 529  
 Bahcall, J. N., & Soneira, R. M. 1981, *ApJ*, 246, 122  
 Bate, M. R. 2000, *MNRAS*, 314, 33  
 Beuzit, J.-L. *et al.* 2004, *A&A*, 425, 997  
 Chanamé, J., & Gould, A. 2004, *ApJ*, 601, 289  
 Chiba, M., & Beers, T. C. 2000, *AJ*, 119, 2843  
 Close, L. M., Richer, H. B., Crabtree, D. R. 1990, *AJ*, 100, 1968  
 Delfosse, X., Forveille, T., Beuzit, J.-L., Udry, S., Mayor, M., Perrier, C. 1999, *A&A*, 344, 897  
 Delgado-Donate, E. J., Clarke, C. J., Bate, M. R., & Hodgkin, S. T. 2004, *MNRAS*, 351, 617  
 Duquennoy, A., & Mayor, M. 1992, *A&A*, 248, 485  
 Fisher, D. A., & Marcy, G. W. 1992, *ApJ*, 396, 178  
 Fuchs, B., & Jahreiss, H. 1998, *A&A*, 329, 81  
 Garnavich, P. M. 1988, *ApJ*, 335, L47  
 Gizis, J. E. 1997, *AJ*, 113, 806  
 Goldberg, D., Mazeh, T., & Latham, D. W. 2003, *ApJ*, 591, 397  
 Goodwin, S. P., & Kroupa, P. 2006, *astro-ph/0603233*  
 Gould, A., Bahcall, J. N., Maoz, D., & Yanny, B. 1995, *ApJ*, 441, 200  
 Gould, A., & Salim, S. 2003, *ApJ*, 582, 1001  
 Gould, A., & Chanamé, J. 2004, *ApJS*, 150, 455  
 Greaves, J. 2004, *MNRAS*, 355, 585  
 Halbwachs, J. L., Mayor, M., Udry, S., Arenou, F. 2003, *A&A*, 397, 159  
 Klein, R. I., Fisher, R. T., Krumholz, M. R., & McKee, C. F. 2003, *RevMexAA*, 15, 92  
 Latham, D. W., Tonry, J., Bahcall, J. N., Soneira, R. M., & Schechter, P. 1984, *ApJ*, 281, L41  
 Latham, David W., Stefanik, Robert P., Torres, Guillermo, Davis, Robert J., Mazeh, Tsevi, Carney, Bruce W., Laird, John B., Morse, Jon A. 2006, *AJ*, 124, 1144  
 Law, N. M., Mackay, C. D., & Baldwin, J. E. 2006, *A&A*, 446, 739  
 Lépine, S., Shara, M. M., & Rich, R. M. 2002, *AJ*, 123, 3434  
 Lépine, S., Rich, R. M. & Shara, M. M. 2003, *AJ*, 125, 1598  
 Lépine, S., & Shara, M. M. 2005, *AJ*, 129, 1483  
 Lépine, S. 2005, *AJ*, 130, 1680  
 Luyten W. J. 1979, *New Luyten Catalogue of stars with proper motions larger than two tenths of an arcsecond (NLTT)*, University of Minnesota, Minneapolis  
 Luyten, W. J. 1987, *The LDS Catalogue: Double Stars with Common Proper Motion*, *Publ. Astr. Obs. Univ. Minnesota III*, part 3, 35; Proper motion survey with the 48-inch Schmidt Telescope, XXI, XXV, XIX, XL, L, LXIV, LV, LXXI, *Univ. Minnes. (1940-1987)*  
 Luyten, W. J. 1988, *Ap&SS*, 142, 17  
 Mallada, E. H., & Fernandez, J. A. 2001, *RevMexAA*, 11, 27  
 Monet, D. G., *et al.* 1998, *The USNO-A2.0 Catalogue*, U.S. Naval Observatory Flagstaff Station (USNOFS) and Universities Space Research Association (USRA) – *CDS-ViZier catalog number I/252*  
 Monet, D. G., Dahn, C. C., Vrba, F. J., Harris, H. C., Pier, J. R., Luginbuhl, C. B., Ables, H. D. 1992, *AJ*, 103, 638  
 Öpik, E. J. 1924, *Tartu Observatory Publications*, 25  
 Poveda, A., & Allen, C. 2004, *RevMexAA*, 21, 49  
 Saarinen, S., & Gilmore, G. 1989, *MNRAS*, 237, 311  
 Salim, S., & Gould, A. 2002, *ApJ*, 575, L83  
 Salim, S., & Gould, A. 2003, *ApJ*, 582, 1011  
 Schuster, W. J., & Nissen, P. E. 1989, *A&A*, 222, 69  
 Skrutskie, M. F., *et al.* 1997, in *The Impact of Large-Scale Near-IR Sky Survey*, ed. F. Garzon *et al.* (Kluwer: Dordrecht), 187  
 Reid, I. N., Gizis, J. E., Hawley, S. L. 2002, *AJ*, 124, 2721  
 Retterer, J. M., & King, I. R. 1982, *ApJ*, 254, 214  
 Weinberg, M. D., Shapiro, S. L., & Wasserman, I. 1987, *ApJ*, 312, 367  
 Weis, E. W. 1984, *ApJS*, 55, 289

TABLE 1  
COMMON PROPER MOTION SYSTEMS WITH 2 OR MORE *Hipparcos* STARS<sup>a</sup>

Primary											Secondary/Tertiary											notes <sup>b</sup>
LSPM	HIP	R.A.	Decl.	$\mu_{R.A.}$ " yr <sup>-1</sup>	$\mu_{Decl.}$ " yr <sup>-1</sup>	V mag	V-J mag	$\pi$ mas	$\pi_{err}$ mas	$\Delta\theta$ "	LSPM	HIP	R.A.	Decl.	$\mu_{R.A.}$ " yr <sup>-1</sup>	$\mu_{Decl.}$ " yr <sup>-1</sup>	V mag	V-J mag	$\pi$ mas	$\pi_{err}$ mas	(22)	
J0005+1804W	495	1.481144	18.075895	-0.146	-0.146	9.22	2.13	25.8	2.1	3.5	J0005+1804E	495	1.481890	18.075220	-0.154	-0.154	9.55	2.43	25.8	2.1	T	
J0005+1814	493	1.478123	18.235014	-0.149	-0.151	7.47	1.14	26.2	0.8	572.9	J0005+1804W	495	1.481144	18.075895	-0.146	-0.146	9.22	2.13	25.8	2.1	T	
J0005+4548N	473	1.420888	45.812080	0.879	-0.154	8.83	2.73	85.1	2.7	328.0	J0005+4547	428	1.295397	45.786568	0.870	-0.151	10.05	3.35	87.0	1.4	T	
J0005+4548N	473	1.420888	45.812080	0.879	-0.154	8.83	2.73	85.1	2.7	6.1	J0005+4548S	473	1.420823	45.810383	0.839	-0.162	8.97	2.83	85.1	2.7	T	
J0032+6714N	2552	8.122603	67.235619	1.741	-0.247	10.49	3.65	98.7	3.4	3.7	J0032+6714S	2552	8.123230	67.234619	1.705	-0.315	12.19	5.02	98.7	3.4		
J0036+2959S	2844	9.009863	29.993027	0.191	-0.403	8.32	1.29	18.9	1.7	6.1	J0036+2959N	2844	9.010551	29.994621	0.177	-0.388	8.98	1.19	18.9	1.7		
J0049+5748	3821	12.276213	57.815186	1.087	-0.560	3.45	1.34	168.0	0.6	12.8	J0049+5749	3821	12.271529	57.817715	1.105	-0.493	7.36	0.19	168.0	0.6		
J0105+1523N	5110	16.374641	15.390063	0.009	-0.196	9.12	2.00	37.6	2.0	6.1	J0105+1523S	5110	16.373962	15.388507	0.006	-0.194	9.80	2.65	37.6	2.0	GC	
J0120+3637N	6240	20.018244	36.630920	-0.103	-0.142	8.87	0.96	15.4	2.0	4.9	J0120+3637S	6240	20.018011	36.629581	-0.109	-0.154	9.73	1.83	15.4	2.0		
J0122+1245S	6431	20.652483	12.750941	0.400	0.008	9.51	1.65	23.8	2.1	5.8	J0122+1245N	6431	20.653130	12.752419	0.403	0.009	11.75	3.07	23.8	2.1		
J0125+3132E	6675	21.410614	31.546171	0.155	-0.050	7.99	1.15	17.3	1.0	56.7	J0125+3133	6668	21.392822	31.550421	0.158	-0.048	8.03	1.10	16.6	1.5	T	
J0125+3133	6668	21.392822	31.550421	0.158	-0.048	8.03	1.10	16.6	1.5	4.6	J0125+3132W	6668	21.391500	31.549845	0.153	-0.048	11.79	3.71	16.6	1.5	T	

<sup>a</sup> The complete table of 168 lines is available in the electronic version of the *Astronomical Journal*. The first 12 lines are shown here as a guide to the contents of the full table.

<sup>b</sup> T: star in a common proper motion triple system, Q: star in a common proper motion quadruple system, GC: star listed in the Gould & Chanamé (2004) catalog of common proper motion double.



TABLE 2  
COMMON PROPER MOTION SYSTEMS WITH ONLY ONE *Hipparcos* STARS, UNCERTAIN COMPANIONSHIP

Primary											Secondary/Tertiary							notes
LSPM	HIP	R.A.	Decl.	$\mu_{RA}$ " yr <sup>-1</sup>	$\mu_{Decl}$ " yr <sup>-1</sup>	V mag	V-J mag	$\pi$ mas	$\pi_{err}$ mas	$\Delta\theta$	LSPM	R.A.	Decl.	$\mu_{RA}$ " yr <sup>-1</sup>	$\mu_{Decl}$ " yr <sup>-1</sup>	V mag	V-J mag	
(1)	(2)	(3)	(4)	(5)	(6)	(7)	(8)	(9)	(10)	(11)	(12)	(13)	(14)	(15)	(16)	(17)	(18)	(19)
J0005+1804W	495	1.481144	18.075895	-0.146	-0.146	9.22	2.13	25.8	2.1	1480.7	J0004+1803	1.049166	18.052927	-0.146	-0.146	16.58	2.51	background/subdwarf
J0300+0517	14054	45.240772	5.287946	0.190	-0.094	8.14	1.58	11.7	1.3	359.4	J0300+0520	45.152958	5.336117	0.189	-0.090	19.10	3.99	background/subdwarf
J0316+5810N	15220	49.058128	58.168789	0.436	-0.305	11.25	3.75	74.3	6.3	1168.9	J0315+5751	48.872692	57.859173	0.467	-0.237	15.57	4.45	background/subdwarf
J0320+4358N	15591	50.203442	43.978798	0.137	-0.118	8.82	1.25	15.1	1.2	44.8	J0320+4358S	50.212368	43.968155	0.137	-0.118	19.70	3.60	background/subdwarf
J0450+6319N	22498	72.604561	63.332939	0.220	-0.196	9.78	2.23	42.6	17.8	40.8	J0450+6319S	72.589020	63.324009	0.236	-0.196	12.70	2.67	background/subdwarf
J0722+0849S	35756	110.631073	8.820297	0.154	-0.265	10.46	1.14	5.9	2.1	34.0	J0722+0849N	110.624702	8.827321	0.149	-0.267	16.66	2.70	subdwarf
J0734+3153E	36850	113.650436	31.888498	-0.200	-0.146	2.96	1.63	63.3	1.2	70.5	J0734+3152	113.656021	31.869511	-0.203	-0.094	9.63	3.56	foreground/double
J0734+3153W	36850	113.649521	31.888388	-0.174	-0.102	1.88	-1.93	63.3	1.2	70.8	J0734+3152	113.656021	31.869511	-0.203	-0.094	9.63	3.56	foreground/double
J0821+3418W	40942	125.336388	34.309975	-0.119	-0.111	8.52	0.55	23.1	1.2	72.9	J0821+3418N	125.360886	34.310619	-0.111	-0.116	17.46	2.52	background/subdwarf
J1106+1415	54299	166.631561	14.262381	0.208	-0.314	9.32	2.24	9.3	2.2	669.3	J1105+1412E	166.447083	14.211407	0.197	-0.327	18.80	5.96	foreground/double
J1425+5151	70497	216.299164	51.850765	-0.237	-0.399	4.05	0.87	68.6	0.6	69.5	J1425+5149	216.298294	51.831474	-0.243	-0.404	13.23	5.35	foreground/double
J1507+7612	74045	226.984421	76.200737	-0.131	0.164	8.73	1.90	34.0	0.7	116.5	J1507+7613	226.988403	76.233093	-0.123	0.157	14.27	5.04	foreground/double
J1543+1101S	76972	235.753250	11.017673	-0.160	0.163	9.02	1.07	7.9	1.7	43.3	J1543+1101N	235.751511	11.029566	-0.144	0.143	17.98	5.32	GC,foreground/double
J1604+3909E	78775	241.236649	39.156509	-0.572	0.052	6.66	1.48	69.6	0.6	70.3	J1604+3909W	241.211884	39.160019	-0.547	0.055	12.86	2.96	GC,background/subdwarf
J1605+3500	78859	241.468567	35.006042	-0.059	-0.251	8.06	1.15	17.1	0.8	42.6	J1605+3459	241.456970	34.999004	-0.041	-0.242	15.32	3.06	background/subdwarf
J1746+2743E	86974	266.614655	27.720701	-0.310	-0.750	3.41	1.54	119.1	0.6	34.2	J1746+2743W	266.604828	27.716873	-0.333	-0.753	10.10	4.33	GC,foreground/double
J1803+8408N	88435	270.834686	84.147728	-0.125	0.137	11.23	2.08	17.5	3.3	30.9	J1803+8408S	270.860107	84.139549	-0.123	0.135	17.18	3.39	background/subdwarf
J2109+5421	104426	317.306641	54.353336	0.184	-0.071	9.87	1.92	22.2	1.1	113.7	J2109+5422	317.330933	54.381577	0.191	-0.073	14.74	4.73	foreground/double
J2114+3802	104887	318.697754	38.045372	0.159	0.431	3.74	0.86	47.8	0.6	534.3	J2115+3804	318.881775	38.077732	0.216	0.453	16.02	3.05	background/subdwarf
J2227+4029	110865	336.924835	40.484993	0.170	0.035	10.82	1.84	13.1	2.4	116.7	J2227+4027	336.940277	40.454769	0.162	0.027	17.77	5.58	foreground/double

TABLE 3  
COMMON PROPER MOTION SYSTEMS WITH ONLY ONE *Hipparcos* STARS<sup>a</sup>

Primary											Secondary/Tertiary						notes <sup>b</sup>	
LSPM	HIP	R.A.	Decl.	$\mu_{R.A.}$ '' yr <sup>-1</sup>	$\mu_{Decl.}$ '' yr <sup>-1</sup>	V mag	V-J mag	$\pi$ mas	$\pi_{err}$ mas	$\Delta\theta$	LSPM	R.A.	Decl.	$\mu_{R.A.}$ '' yr <sup>-1</sup>	$\mu_{Decl.}$ '' yr <sup>-1</sup>	V mag		V-J mag
(1)	(2)	(3)	(4)	(5)	(6)	(7)	(8)	(9)	(10)	(11)	(12)	(13)	(14)	(15)	(16)	(17)	(18)	(19)
J0006+0549W	538	1.632458	5.825399	0.195	0.040	11.05	1.84	13.3	2.4	23.4	J0006+0549E	1.637383	5.821126	0.195	0.041	16.63	4.73	
J0009+2516E	754	2.315609	25.281969	0.173	-0.149	7.78	1.29	22.1	2.3	29.6	J0009+2516W	2.307973	25.277500	0.166	-0.145	10.94	2.10	GC
J0009+2739	731	2.262073	27.651577	0.215	0.144	11.80	2.38	22.5	3.0	68.9	J0008+2739	2.248174	27.666235	0.215	0.144	13.70	3.27	GC
J0010+4806W	889	2.733613	48.110405	0.169	0.000	8.41	1.04	16.5	0.9	23.9	J0010+4806E	2.740871	48.114941	0.168	0.003	10.72	1.87	
J0012+2142N	1006	3.139525	21.713451	0.183	-0.289	11.91	3.07	34.5	11.7	29.0	J0012+2142S	3.143580	21.706341	0.187	-0.294	13.65	3.99	
J0013+8039W	1092	3.411198	80.665802	0.253	0.185	11.15	3.39	51.1	3.3	12.9	J0013+8039E	3.429084	80.663689	0.259	0.193	16.88	5.94	GC
J0015+5304S	1224	3.811452	53.074158	0.220	0.044	10.41	1.57	12.2	2.1	18.8	J0015+5304N	3.810659	53.079353	0.232	0.005	14.34	3.52	GC
J0016+1951W	1295	4.060917	19.860455	0.709	-0.748	11.85	3.97	49.9	21.6	25.1	J0016+1951E	4.067259	19.864059	0.709	-0.748	13.55	4.66	
J0018+4401W	1475	4.595309	44.022949	2.888	0.409	8.15	2.90	280.3	1.0	36.0	J0018+4401E	4.607785	44.027344	2.912	0.351	11.12	4.33	GC
J0023+7711W	1860	5.870120	77.189301	-0.838	0.045	11.53	3.49	50.7	2.7	11.3	J0023+7711E	5.882650	77.190758	-0.838	0.045	15.17	5.24	GC
J0033+4443	2600	8.255900	44.730080	0.222	-0.044	10.29	1.48	9.5	1.6	28.9	J0033+4444	8.261676	44.736973	0.220	-0.049	16.85	0.18	GC
J0038+4259W	3022	9.621646	42.999924	0.192	-0.083	9.95	1.54	19.9	1.9	53.1	J0038+4259E	9.638277	42.991577	0.194	-0.079	13.54	3.05	GC

<sup>a</sup> The complete table of 364 lines is available in the electronic version of the *Astronomical Journal*. The first 12 lines are shown here as a guide to the contents of the full table.

<sup>b</sup> T: star in a common proper motion triple system, Q: star in a common proper motion quadruple system, GC: star listed in the Gould & Chanamé (2004) catalog of common proper motion double.